Essence of Earthquake Resistant Design of Port Facilities

- Regulations and Recommendations –

Independent Administrative Institution Port and Airport Research Institute

1. Introduction

The design standard for port facilities in Japan went through a major revision in 2007. The most remarkable feature of the new design standard is that it is completely based on the idea of “performance-based design”. At the same time, the new standard is designed to be consistent with recent advances in the field of engineering seismology and earthquake engineering. The purpose of this article is to present the essence of the earthquake resistant design, which is a part of the new design standard. The complete version of the design standard in Japanese is available from the Japan Ports and Harbours Association (www.phaj.or.jp) and the semi-complete version in English will be available from the Overseas Coastal Area Development Institute of Japan (www.ocdi.or.jp/en/index.html).

The idea of “performance-based design” constitutes the backbone of the new design standard. The structure of the design standard could be described as Figure 1. The objective of the facility is at the top of the structure. Then, the performance requirements are specified in the “ministerial ordinance” to achieve the objective of the facility, in a plain language so that they can be understood by taxpayers. Thirdly, the performance criteria are defined in the “notification” to achieve the performance requirements, using technical terms so that they can be strictly interpreted by engineers. The “ministerial ordinance” and the “notification” are supplemented by the “commentaries”. All of these are regulatory. Finally, the performance of the facility is verified by some verification method. In principle, there is no restriction in the selection of the method of verification as far as the method is appropriate. Recommended verification methods are described in the annexes of the design standard for the convenience of the engineers. The annexes are informative and not regulatory.

N.B. In the following, the footnotes were given by the author of this article and they are not included in the design standard.

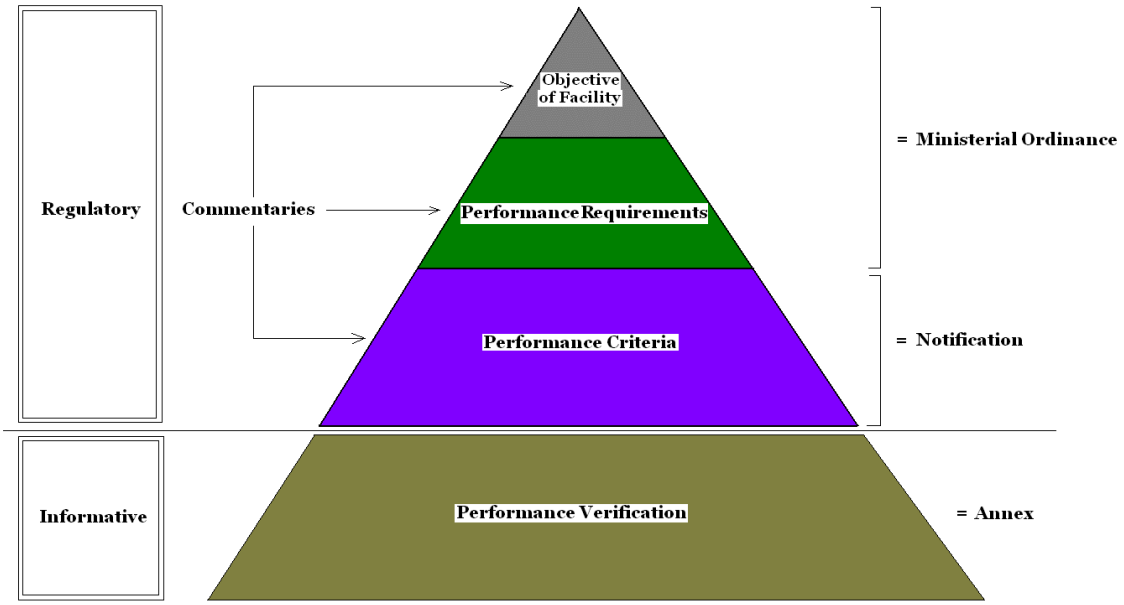

Figure 1 Structure of the design standard

2. Design Ground Motions

[Ministerial Ordinance] (Definitions)
Article 1
(1) The L1 ground motion is defined as a ground motion with high probability of occurrence at the site during the design working life.
(2) The L2 ground motion is defined as the largest ground motion among ground motions at the site from scenario earthquakes.

[Notification] (Design Ground Motions)
Article 16
(1) The L1 ground motion shall be determined appropriately as a stochastic time history with considerations of source, path and site effects, based on the results of earthquake observation.
(2) The L2 ground motion shall be determined appropriately as a time history with considerations of source, path and site effects, based on the results of earthquake observation and the source parameters of the scenario earthquake.

[Commentary]
(1) The depth at which the design ground motions are specified
The design ground motions should be specified at the outcrop of a firm ground, which is defined in (2). If a ground motion at another depth is needed for the performance verification, it should be obtained from the design ground motion at the outcrop of the firm ground, using some appropriate method including 1D response analysis of the local soil deposit.
(2) The firm ground
A soil layer is defined as the firm ground if all layers below the layer belong to one of the following.
- Rock.
- Sandy soil with SPT N value over 50.
- Cohesive soil with q_u over 650 kN/m^2.
- Soil with shear wave velocity over 300 m/s.

(3) The site effect
To evaluate the site effect appropriately, it is necessary to take into account the results of earthquake observation in and around the port.
(4) Time history
The L1 and L2 ground motion should be specified as an acceleration, velocity or displacement time histories.
(5) L1 ground motion
A stochastic time history is defined as a time history of ground motion obtained as a result of a probabilistic seismic hazard analysis, in which the probability of the occurrence of the earthquakes is considered. The Fourier spectrum of the L1 ground motion should follow the uniform-hazard Fourier spectrum, for which the probability of exceedance is constant for all frequencies. In the probabilistic seismic hazard analysis to determine the L1 ground motion, the occurrence of the earthquakes around the port is assumed to follow a Poisson process, that is, past history of the earthquake is neglected. Consequently, the ground motions from huge subduction zone earthquakes along the Nankai Trough would not necessarily be considered as L1 ground motion although their probability of occurrence might be high if their past history is considered[1].
(6) Return period
The return period of the L1 ground motion should be 75 years[2].

[1] The ground motions from huge subduction zone earthquakes along the Nankai Trough would be considered more as candidates for L2 ground motion.
[2] This means that the probability of exceedance is 1/75 a year.

[Commentary]
(7) L2 ground motion

To determine the L2 ground motion, a scenario earthquake should be selected from the following candidate earthquakes (a) – (f), taking into account the amplitude, predominant period and duration of the ground motions generated from each candidate earthquake and their effect on structures.

a) Recurrence of past damaging earthquakes
b) Earthquakes caused by active faults
c) Other earthquakes expected from seismological and/or geological point of view.
d) Scenario earthquakes hypothesized by the branches of Japanese government.
e) Scenario earthquakes hypothesized by the local governments.
f) M6.5 earthquake just beneath the site.

To determine the L2 ground motion, macroscopic and microscopic source parameters of the earthquake should be determined appropriately, taking into account the characteristic of the earthquake.

2.1 General

[Annex]

Generally speaking, strong ground motions are determined by three effects, namely, the source effect, the path effect and the site effect as shown in Figure 2. The source effect is defined as the effect of the rupture process of the earthquake. The path effect is defined as the effect of the materials along the propagation path from the source to the bedrock beneath the site. The site effect is defined as the effect of sediments below the site down to the bedrock. The bedrock is defined as a layer with a shear wave velocity over 3000 m/s in this design standard (In many cases it corresponds to fresh granite in Japan).

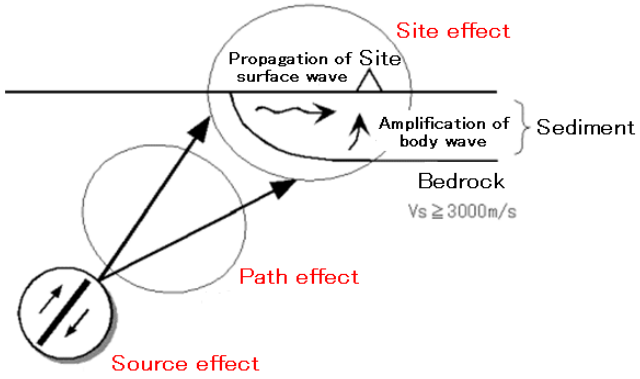

Figure 2 Source, path and site effects

In general, the Fourier amplitude of a ground motion observed at the ground surface $O(f)$ is the product of the source effect $S(f)$, the path effect $P(f)$ and the site effect $G(f)$.

$$O(f) = S(f)P(f)G(f) \tag{1}$$

On the other hand, the group delay time of a ground motion observed at the ground surface $t_{gr}{}^{O}(f)$ is the sum of the source effect $t_{gr}{}^{S}(f)$, the path effect $t_{gr}{}^{P}(f)$ and the site effect $t_{gr}{}^{G}(f)$ (Sawada *et al*., 1998).

$$t_{gr}{}^{O}(f) = t_{gr}{}^{S}(f) + t_{gr}{}^{P}(f) + t_{gr}{}^{G}(f) \tag{2}$$

The group delay time is defined as the derivative of the Fourier phase with respect to angular frequency and

it roughly corresponds to the arrival time of each frequency component. In this article, the amplification of Fourier amplitude spectrum caused by the sediment is called “the site amplification factor”.

2.1.1 Source Effect

(1) Source spectrum

According to the ω^{-2} model (Aki, 1967), the acceleration Fourier amplitude spectrum of a seismic wave radiated from a fault (source spectrum) can be expressed as follows.

$$S(f) = C \frac{M_0}{4\pi\rho V_S^3} \frac{(2\pi f)^2}{1+(f/f_c)^2} \tag{3}$$

where

M_0: seismic moment
f_c: corner frequency
ρ : density in the bedrock
V_s: shear wave velocity in the bedrock
C: constant (to be described later)

The seismic moment is defined as follows (Aki, 1966).

$$M_0 = \mu A D_0 \tag{4}$$

where

μ : rigidity in the bedrock
A: area of the fault
D_0: slip on the fault

Figure 3 shows the displacement, velocity and acceleration source spectra following the ω^{-2} model.

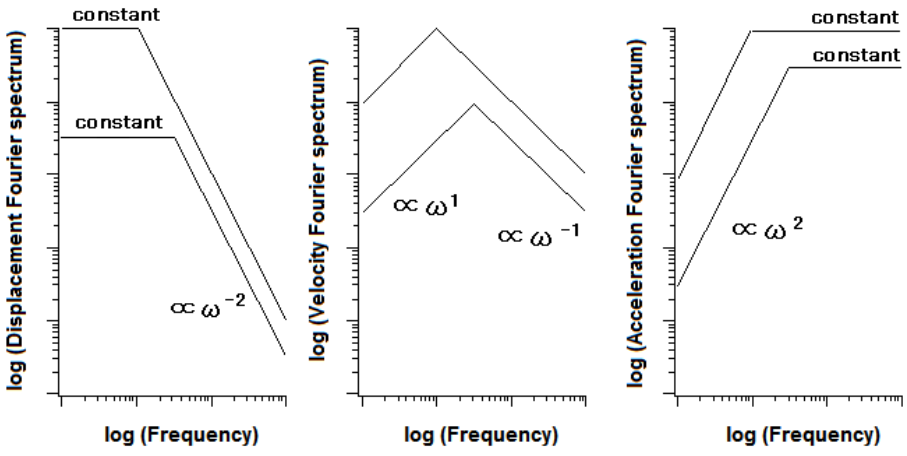

Figure 3 Source spectra which follow the ω^{-2} model.

(2) Forward directivity effect

The source of an earthquake is not a point but a fault with a finite dimension. The rupture of the fault starts from one point and propagates on the fault at a finite velocity. Because the rupture velocity is not very

different from the shear wave velocity, at the site in the direction of rupture propagation, seismic waves radiated from each part of the fault are superposed coherently and produce a large pulse-like ground motion. This phenomenon is called “the forward directivity effect”. In the case of the 1995 Hyogo-ken Nanbu earthquake, the rupture started beneath the Akashi strait and propagated toward Kobe City as well as Awaji Island, causing serious damage to Kobe City. At the same time, it has been recognized that, when the amplitude of the ground motion becomes large due to the forward directivity effect, the component perpendicular to the strike of the fault tend to be larger. This characteristic can be utilized in the port planning. If a quay wall is oriented perpendicular to the strike of a nearby active fault, then it will be less affected by the ground motion even when the site of the quay wall is subject to a forward directivity effect (Nozu and Iwan, 2003).

(3) Asperity

It has been revealed that the slip on the fault of a large earthquake is not uniform and there is a relatively small region called “asperities” in which the slip (and the slip velocity) is especially large. To reproduce the recorded ground motions in the past earthquakes appropriately, it is necessary to take into account the existence of asperities[3]. The characteristic source model is defined as a source model composed of rectangular asperities, within which the slip and the slip velocity is uniform.

[3] Figure 3.1 (left) shows the characteristic source model by Yamada *et al.* (1999) for the 1995 Hyogo-ken Nanbu earthquake. Figure 3.1 (right) shows its cross section for the Kobe side. The source model has three asperities in the Kobe side. The stars indicate the rupture starting point for each asperity. The synthetic ground motions produced from this source model with the Kowada’s (1998) method (to be described later) agree quite well with the observed ones (Figure 3.2), indicating the importance of the existence of asperities. See Nozu and sugano (2008) and Nozu *et al.* (2008) for more information.

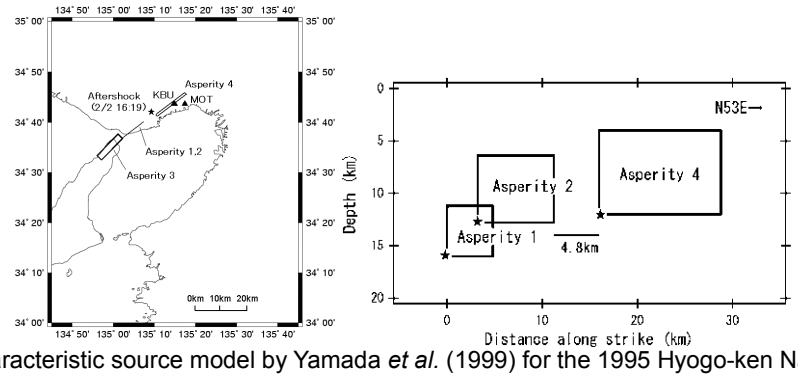

Figure 3.1 Characteristic source model by Yamada *et al.* (1999) for the 1995 Hyogo-ken Nanbu earthquake

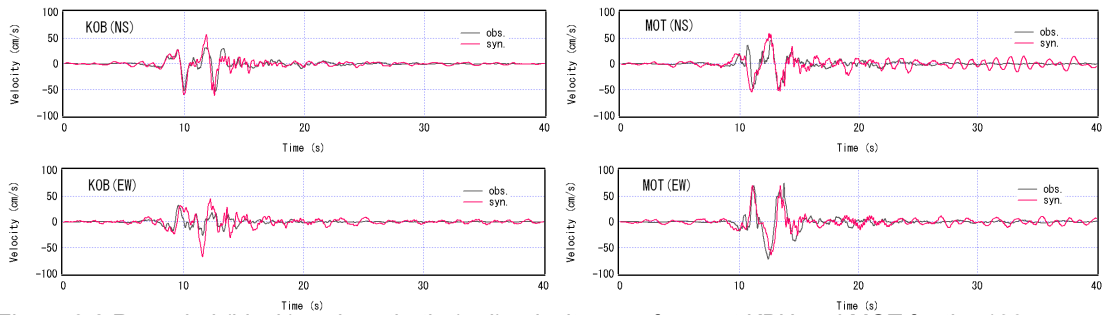

Figure 3.2 Recorded (black) and synthetic (red) velocity waveforms at KBU and MOT for the 1995 Hyogo-ken Nanbu earthquake.

2.1.2 Path Effect

As for the path effect, it is a common practice to take into account both the geometrical spreading and the inelastic damping as follows.

$$P(f) = \frac{1}{r}\exp(-\pi f r / Q V_S) \tag{5}$$

where

r: hypocentral distance
Q: Q value along the propagation path

2.1.3 Site Effect

The existence of sediments below the site has significant effects on the amplitude, the frequency content and the duration of strong ground motions[4]. Figure 4 shows an example of the effect of the sediments on the frequency content of strong ground motions. At Hachinohe Port, both of the Fourier spectra from the 1968 Tokachi-oki earthquake (M_J=7.9) and the 1994 Sanriku Haruka-oki earthquake (M_J=7.5) are characterized by a peak at 2.5 seconds. The former record is famous as the Hachinohe wave and has been widely used for the design of port structures in Japan. On the other hand, at Kansai International Airport, both of the Fourier spectra from the 1995 Hyogo-ken Nanbu earthquake (M_J=7.3) and the 2000 Tottori-ken Seibu earthquake (M_J=7.3) are characterized by a peak at 5 seconds. The difference of predominant periods can be attributed to the thickness of sediments down to the bedrock at each observation station.

[4] Figure 4.1 shows an example of the importance of the site effect. The left panel shows the topography around the Port of Sakai, west Japan. Two observation stations, namely, Sakaiminato-G (Strong Motion Earthquake Observation in Japanese Ports) and JMA (the Japan Meteorological Agency) are located in the plains of Yumigahama Peninsula. Other two stations, namely, SMN001 of K-NET (Kinoshita, 1998) and SMNH10 of KiK-net (Aoi *et al.*, 2000) are located in mountainous Shimane Peninsula. Observed peak ground velocities during the 2000 Tottori-ken Seibu earthquake (M_J7.3) were approximately four times larger for the plains of Yumigahama Peninsula than for mountainous Shimane Peninsula (Figure 4.1). Thus, evaluation of the site effect is fundamentally important to predict strong ground motions from future large earthquakes and to determine design ground motions.

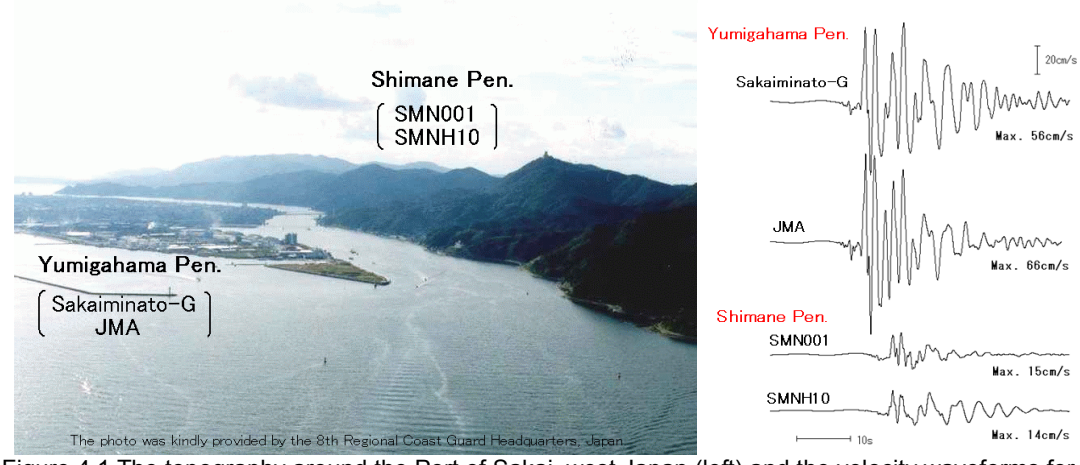

Figure 4.1 The topography around the Port of Sakai, west Japan (left) and the velocity waveforms for the fault-normal component recorded around the port during the 2000 Tottori-ken Seibu earthquake (M_J7.3).

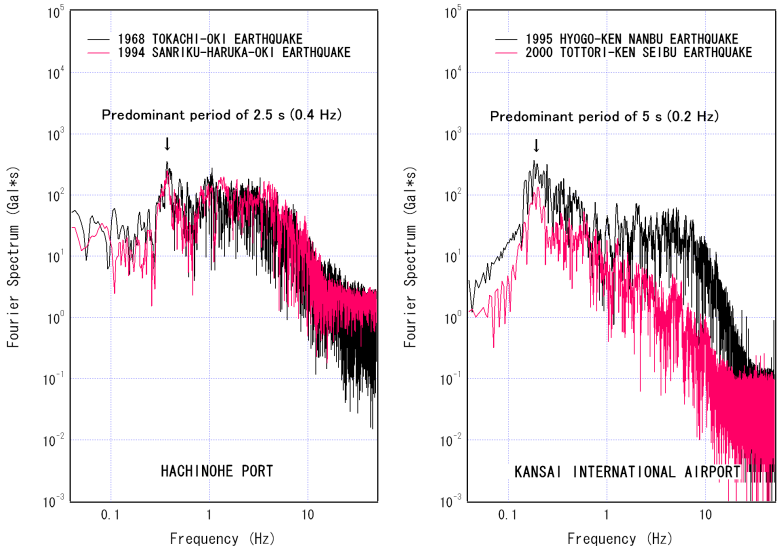

Figure 4 Fourier spectra of past major strong motion records obtained at Hachinohe Port (NS component) and Kansai International Airport (Runway-normal component)

2.1.4 Nonlinear Response of Local Soil Deposit

In general, the material properties of local soft soil deposit are dependent on the strain level. When it is subject to a strong ground motion, the shear modulus decreases and the damping factor increases. This phenomenon is referred to as the nonlinear behavior of the local soft soil deposit. Evidence for the nonlinear behavior of the local soft soil deposit can be found in the strong motion records at vertical array stations. Figure 5 shows the surface-to-borehole Fourier spectral ratios at the vertical array station at Kushiro Port for all earthquakes with M≥5 in 2003. All the spectral ratios have peaks at 1 Hz and 3 Hz, except for the 2003 Tokachi-oki earthquake (M_J8.0), for which the peaks are shifted to lower frequencies, indicating the nonlinear behavior of the local soft soil deposit.

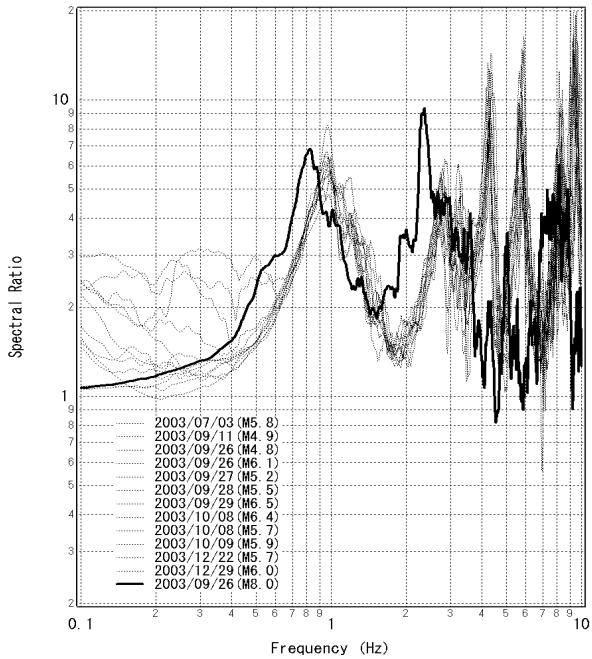

Figure 5 Fourier spectral ratios (Surface/GL-77m) at the vertical array station at Kushiro Port (Fourier spectra are the root mean square of the two horizontal components)

2.2 L1 Ground Motion

2.2.1 General

The L1 ground motion should be determined based on the probabilistic seismic hazard analysis, taking into account the source effect, the path effect and the site effect (from the bedrock to the outcrop of the firm ground). The L1 ground motion should be specified at the outcrop of the firm ground. The L1 ground motions for major ports in Japan evaluated by the National Institute for Land and Infrastructure Management are available from its website (http://www.ysk.nilim.go.jp/kakubu/kouwan/sisetu/sisetu.html).

2.2.2 Evaluation of Site Amplification Factor

The site amplification factor to determine the design ground motion should be evaluated from the seismograms obtained at a station of earthquake observation in and around the port after making sure by microtremor observations that the characteristics of ground motions do not differ significantly between the site of construction and the observation station. If the characteristics of ground motions are found to be different between them, it is recommended to conduct a temporal earthquake observation at the site of construction to evaluate the site amplification factor. The site amplification factor evaluated from a seismogram usually represents the amplification factor from the bedrock to the ground surface because the seismometer is located at the ground surface in many cases[5]. The site amplification factor (from the bedrock to the outcrop of the firm ground) can be obtained by dividing the site amplification factor (from the bedrock to the ground surface) by the transfer function (from the outcrop of the firm ground to the ground surface), which is typically evaluated by the linear multiple reflection theory.

(1) Temporal earthquake observation

The term for the temporal observation should be determined taking into account the seismicity of the area. Typically, in Japan's case, a term of 1-3 years would be required. The seismometers used for the observation should cover all the frequency range for which strong ground motions should be predicted. The trigger level should be chosen very carefully. In general, a very small trigger level should be chosen to obtain as many records as possible in a limited term. It might be useful to adopt a mechanism in which the seismometer is triggered when the velocity, instead of the acceleration, exceeds certain value. The location of the observation should also be determined carefully. When it is difficult to install the seismometer just at the construction site, then microtremor observation should be conducted in and around the construction site and the seismometer should be installed within an area in which the characteristics of microtremor can be regarded uniform.

(2) Spectral inversion

The spectral inversion (Iwata and Irikura, 1986) is one of the methods to evaluate the site amplification factor at earthquake observation stations. Let us assume that the ground motions from M earthquakes have been observed at N stations. Then the Fourier spectra of the observed ground motions can be represented as the product of the source effect, the path effect and the site effect as follows.

$$O_{ij}(f) = S_i(f) P_{ij}(f) G_j(f) \tag{6}$$

where

O_{ij}(f): Fourier spectrum of the record from the i^{th} earthquake at the j^{th} station.
S_i(f): Source effect (source spectrum) for the i^{th} earthquake.
P_{ij}(f): Path effect from the i^{th} earthquake to the j^{th} station.

[5] It is not recommended to use a borehole record to evaluate site amplification factors because the Fourier spectrum of a borehole record has a hole due to the interference of upcoming and downgoing waves.

G_j(f): Site effect for the j^{th} station.

The path effect can be represented as follows, taking into account the geometrical spreading and the inelastic damping.

$$P_{ij}(f) = \frac{1}{r_{ij}} \exp\left(-\pi f r_{ij} / Q V_S\right) \tag{7}$$

where

r: distance from the i^{th} earthquake to the j^{th} station
Q: Q value along the propagation path.

By substituting the equation (7) into the equation (6) and taking the natural logarithm, one obtains

$$\log O_{ij} = -\log r_{ij} + \log S_i + \log G_j - (\log e)\pi f r_{ij} / Q V_S \tag{8}$$

In general, the numbers of the unknowns included in the equation (8) is smaller than the number of the equations, *i.e.*, the number of the records. Thus one can solve the equation (8) by using the least square method. It should be noted, however, that the least square solutions of the equation (8) are not unique. For instance, if S_i and G_j are the least square solutions, $S_i/2$ and $2G_j$ will also be the least square solutions. Thus, in this analysis, an additional constraint is required. As for this constraint, it is recommended to select a frequency-dependent reference site for which the site amplification factor is smallest among all the sites with averaged shear wave velocity over 400 m/s at top 10 m and to assume that the site amplification factor is unity for this reference site (Nozu and Nagao, 2005). It is also recommended to make sure that the seismic moments estimated from the solutions of the equation (8) are in agreement with those of CMT solutions on the average. Other recommendations on the spectral inversion can be summarized as follows.

- It is preferable to avoid records with epicentral distances larger than 150 - 200 km because the equation (7) is not applicable to long-distance records.
- It is preferable to avoid records from earthquakes with M≥6 because it is not appropriate to assume a azimuth-independent source effect S_i for large earthquakes.
- It is preferable to avoid records from earthquakes with M<4.5 because, for small earthquakes, the signal-to-noise ratio at low frequencies tends to be insufficient[6].
- It is preferable to avoid records with large amplitude to avoid the effects of soil nonlinearity.

The digital data of the site amplification factors at earthquake observation stations in Japan evaluated by the Port and Airport Research Institute and the National Institute for Land and Infrastructure Management are available on a CD-ROM (Nozu and Nagao, 2005).

(3) Evaluation of site amplification factors at a temporary station

Based on the known site amplification factors at permanent stations, the site amplification factor at a temporary station can be evaluated as follows. The first step is to find earthquakes which are recorded both at the temporary station and the surrounding permanent stations. Then, for these earthquakes, the source spectra should be determined so that the equation (6) is satisfied for the permanent stations. It is a common practice to assume that the source spectra follow the ω^{-2} model (the equation (3)). Finally, using the source spectra thus obtained and the observed spectra at the temporary station, the site amplification factor at the temporary station can be determined from the equation (6).

[6] To evaluate appropriate design ground motions for port facilities, the site amplification factor should sufficiently be accurate down to 0.2 Hz.

A simplified version of this analysis can be applied if the temporary station is very close to a permanent station for which the site amplification factor is known. In this case, these stations share the same source effect and the same path effect. Therefore, the Fourier spectral ratio of the records from the same earthquake at these stations represents the ratio of the site amplification factors. Thus, the site amplification factor for the temporary station can be easily obtained from the spectral ratios.

2.2.3 Probabilistic Seismic Hazard Analysis

In the probabilistic seismic hazard analysis, all the possible earthquake scenarios have to be considered (let us denote by N the number of all the scenarios). For each scenario, the annual probability of occurrence has to be assigned. The scenario earthquakes fall into two categories. One is the scenario earthquakes that are related to particular faults (for example, active faults or plate boundaries). The other is the scenario earthquakes randomly distributed around the site. For the latter type of earthquakes, the earthquake catalogues are used to evaluate the annual probability of occurrence as a function of earthquake magnitude.

For each earthquake scenario, the Fourier amplitude spectrum (at the outcrop of a firm ground) at the site of interest can be evaluated, taking into account the source, path and the site effects. For the randomly distributed scenarios, the source spectrum can be assumed to follow the ω^{-2} model (the equation (3)).

Let us consider one particular frequency for a while. Let n ($<N$) denote the number of scenarios for which the Fourier spectrum at the frequency exceeds a given value X. If we sum up the annual probability of occurrence for the n scenarios, then it will give the annual probability that the Fourier spectrum at the frequency exceeds X. This is called the “annual probability of exceedance” and denoted here as $P(X)$. If $P(X)$ is plotted against X, it is called the “hazard curve”.

Finally, let us find X for which $P(X)=1/75$ and denote it by X_{75}. If we plot X_{75} as a function of frequency, it is called the “uniform hazard Fourier spectrum”. To transform X_{75} back into the time domain, the Fourier phase of a record at the earthquake observation station can be used[7]. The time history thus obtained can be used as the L1 ground motion.

2.3 L2 Ground Motion

2.3.1 General

The L2 ground motion should be determined based on the synthesis of strong ground motions from scenario earthquakes, taking into account the source effect, the path effect and the site effect (from the bedrock to the outcrop of the firm ground). The L2 ground motion should be specified at the outcrop of the firm ground.

2.3.2 Scenario Earthquake

To determine the L2 ground motion, scenario earthquakes which may cause the largest ground motion at the site should be selected from the following earthquakes (a) – (f).

a) Recurrence of past damaging earthquakes
b) Earthquakes caused by active faults
c) Other earthquakes expected from seismological and/or geological point of view.
d) Scenario earthquakes hypothesized by the branches of Japanese government.
e) Scenario earthquakes hypothesized by the local governments.

[7] Because X_{75} corresponds to the outcrop of a firm ground, the Fourier phase at the outcrop of the firm ground should be used.

f) M6.5 earthquake just beneath the site.

Then, strong ground motions at the site from the selected earthquakes should be evaluated, using the source parameters described in **2.3.3** and the method of synthesis described in **2.3.5**. Finally, from the calculated ground motions, the one which has the largest effect on port facilities should be selected as the L2 ground motion.

2.3.3 Source Parameters

The source parameters to be determined fall into three categories: the macroscopic parameters, the microscopic parameters and the other parameters. The macroscopic source parameters include the location of the fault, the strike of the fault, the dip of the fault, the area of the fault and the seismic moment of the fault. The microscopic parameters include the number of the asperities, the area of the asperities, the seismic moment of the asperities, the rise time of the asperities and the location of the asperities. The other parameters include the rupture starting point and the rupture velocity. The meaning of the source parameters are shown in Figure 6.

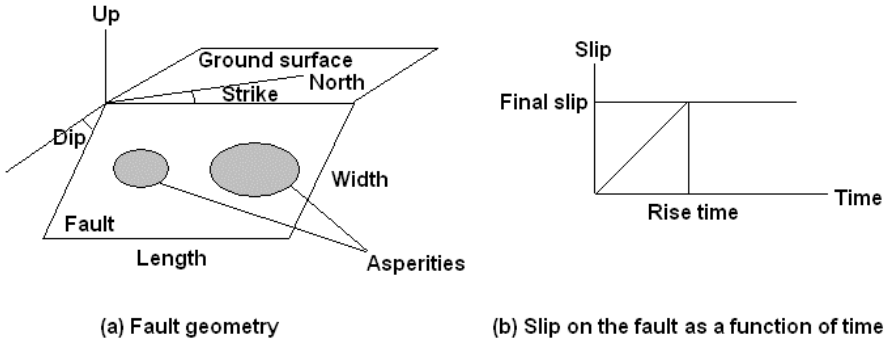

Figure 6 Meaning of the source parameters

There are two choices in determining the source parameters. One is to follow the standard method described below. The other is to determine the source parameters based on detailed seismological, geological and/or geomorphological investigations on the scenario earthquake. The standard method described below depends on the type of the scenario earthquake.

(1) Recurrence of past damaging earthquakes

When the recurrence of a past damaging earthquake is hypothesized, the source parameters which are consistent with strong motion records of the past earthquake can be used if strong motion records are available. For example, source parameters which are consistent with strong motion records are presented by Nozu and Sugano (2008) for the 1968 Tokachi-oki earthquake (M_J7.9), the 1978 Miyagi-ken-oki earthquake (M_J7.5) and the 2003 Tokachi-oki earthquake (M_J8.0). When strong ground motions are not available for the past earthquake, the source parameters which are consistent with seismic intensity of the past earthquake can be used.

(2) Earthquakes caused by active faults

When an earthquake caused by an active fault is hypothesized, the macroscopic fault parameters can be specified as follows. First, the length of the fault, the strike of the fault and the dip of the fault should be determined based on the information on the active fault. The width of the fault should be determined by considering the thickness of seismogenic layers and the dip of the fault. The seismic moment of the earthquake can be estimated from the area of the fault as follows (Somerville *et al.*, 1999).

$$S(\mathrm{km}^2) = 2.23\times10^{-15}\times M_0{}^{2/3}(\mathrm{dyne}\cdot\mathrm{cm}) \quad (9)$$

The microscopic parameters can be determined as follows. First, as for the area of the asperity, 22% of the total area can be assigned to the asperity. If two asperities are considered, 16% and 6% can be assigned to the larger and the smaller asperities, respectively. As for the seismic moment of the asperity, 44% of the total seismic moment can be assigned to the asperity. If two asperities are considered, 36% and 8% can be assigned to the larger and the smaller asperities, respectively. If the magnitude of the earthquake is larger than 7, two asperities should be considered. The rise time of the asperity should be determined from the width of the asperity and the rupture velocity as follows.

$$\tau = \left(W_a/V_r\right)/4 \quad (10)$$

The location of the asperity and the rupture starting point should be specified as Figure 7. The center of the asperity should be 10 km deep and one side of the asperity should be closest to the site. The rupture starting point should be specified so that the rupture propagates towards the site. The rupture velocity can be 80% of the shear wave velocity in the bedrock. When two asperities are considered, at least one of them should be located as Figure 7.

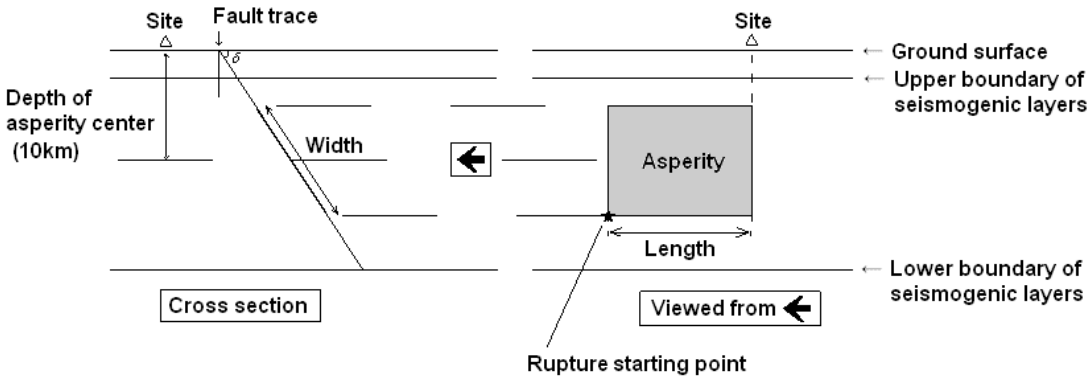

Figure 7 Location of the asperity and the rupture starting point

(3) M6.5 earthquake just beneath the site

When an M6.5 earthquake just beneath the site is hypothesized, the seismic moment of the earthquake can be estimated from the magnitude as follows.

$$\log M_0 = 1.17M + 17.72 \ \ (\mathrm{dyne}\cdot\mathrm{cm}) \quad (11)$$

Then, the equation (9) can be used to determine the area of the fault. The dip of the fault can be 90°. The microscopic parameters and the other parameters can be determined in the same way as those for an earthquake caused by an active fault.

2.3.4 Evaluation of Site Amplification Factor

The description on the site amplification factor for the L1 ground motion (**2.2.2**) applies to the site amplification factor for the L2 ground motion.

2.3.5 Synthesis of Earthquake Ground Motion

There are several reliable methods for the synthesis of earthquake ground motions from the asperities. In this section, the Kowada's method (Kowada, 1998; Nozu and sugano, 2008; Nozu *et al*., 2008) is described.

First, a small earthquake should be hypothesized, whose area is equal to the area of the target asperity divided by N^2 and whose seismic moment is equal to the seismic moment of the target asperity divided by N^3. The ground motion from the small earthquake is called the "Green's function". The Fourier amplitude of the Green's function is evaluated as a product of the source spectrum $|S(f)|$, the path effect $|P(f)|$ and the site amplification factor $|G(f)|$. The source spectrum and the path effect can be specified as follows.

$$S(f) = R_{\theta\phi} FS \cdot PRTITN \cdot \frac{M_{0e}}{4\pi\rho V_S^3} \frac{(2\pi f)^2}{1+(f/f_c)^2} \tag{12}$$

$$P(f) = \frac{1}{r}\exp(-\pi f r / Q V_S) \tag{13}$$

where

M_{0e}: seismic moment of the small event
f_c: corner frequency of the small event
ρ : density in the bedrock
V_S: shear wave velocity in the bedrock
$R_{\theta\phi}$: radiation coefficient (=0.63)
FS: amplification due to free surface (=2)
PRTITN: coefficient representing the partition of seismic energy into two horizontal components
r: hypocentral distance for the small earthquake
Q: Q value along the propagation path.

As for *PRTITN*, values in Table 1 can be used.

Table 1 Standard values for *PRTITN*

	Near source	Not near source
Subduction earthquake	0.71	0.71
Earthquake caused by active fault	0.85 (Strike normal) 0.53 (Strike parallel)	0.71
M6.5 earthquake just beneath the site	0.71	0.71

The corner frequency of the small earthquake can be obtained from the area of the small earthquake S_e as follows (Brune, 1970; Brune, 1971).

$$f_c = 0.66 V_S / \sqrt{S_e} \tag{14}$$

As for the Fourier phase, the Fourier phase of a record at the earthquake observation station can be used[8]. If several records are available at the site, it is recommended to choose an event which has a similar incident angle and a similar backazimuth with the target asperity. The Green's function in the frequency domain can be written as follows.

$$|S(f)|\ |P(f)|\ |G(f)|\ Os(f) / |\ Os(f)|_p, \tag{15}$$

[8] If the site amplification factor from the bedrock to the ground surface is used, the Fourier phase at the ground surface should be used. If the site amplification factor from the bedrock to the outcrop of a firm ground is used, the Fourier phase at the outcrop of the firm ground should be used.

where $Os(f)$ is the Fourier transform of a record at the site and $|Os(f)|_p$ is its Parzen-windowed amplitude (band width of 0.05 Hz is used). The time domain Green's function can be obtained as the inverse Fourier transform of the equation (15). Finally, the time domain Green's function can be superposed as follows (*e.g.*, Miyake *et al.*, 1997).

$$U(t) = \sum_{i=1}^{N}\sum_{j=1}^{N}\left(r/r_{ij}\right) f(t) * u(t - t_{ij})$$

$$f(t) = \delta(t) + \left\{1/n'/\left(1 - e^{-1}\right)\right\} \sum_{k=1}^{(N-1)n'} \left[e^{-(k-1)/(N-1)/n'} \delta\left\{t - (k-1)\tau/(N-1)/n'\right\}\right] \quad (16)$$

$$t_{ij} = \left(r_{ij} - r_0\right)/V_S + \xi_{ij}/V_r$$

where

$U(t)$: Ground motion from the asperity (designated as “large event” in Figure 8)
$u(t)$: Green’s function
$f(t)$: Function to correct for the difference of slip velocity time functions for the asperity and the small earthquake
r: hypocentral distance for the small earthquake
r_{ij}: distance from the subfault ij to the site
τ : Rise time of the asperity
n': integer used to remove artificial periodicity
r_0 : distance from the rupture starting point to the site
ξ_{ij} : distance from the rupture starting point to the subfault ij.
V_S: shear wave velocity in the bedrock
V_r: Rupture velocity

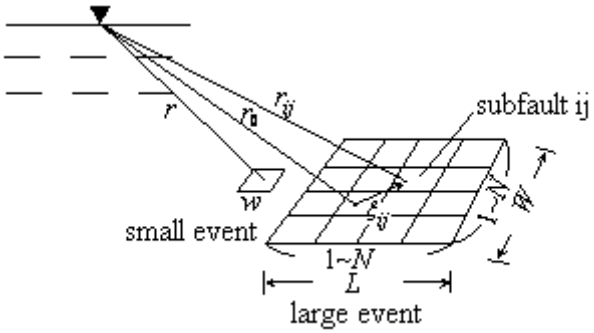

Figure 8 Superposition of Green’s functions

When two or more asperities are considered, contribution from all the asperities should be superposed. The ground motion thus obtained is either at the ground surface or at the outcrop of the firm ground, depending on the site amplification factor used in the equation (15). To obtain the ground motion at the outcrop of the firm ground from the ground motion at the ground surface, the linear multiple reflection theory can be used.

A computer program to synthesize strong ground motions based on the method described above is open to public from the Port and Airport Research Institute (Nozu and Sugano, 2008).

3. Earthquake Resistant Design of Quay Walls

[Ministerial Ordinance] (Performance Requirements for Quay Walls)
Article 26
(1) For the L1 ground motion, ordinary functions of quay walls shall be maintained.
(2) For the L2 ground motion, particular functions expected for the quay wall after the earthquake shall be recovered within a designated period of time in the case of seismic-resistant quay walls. In the case of a seismic-resistant quay wall with higher seismic resistance, particular functions expected for the quay wall after the earthquake shall be maintained.

[Commentary]
Seismic resistant quay walls can be categorized as follows in terms of functions expected after the earthquake and the period in which the functions should be recovered.
(1) Special seismic resistant quay walls (for emergency transportation): A facility which can be used for mooring, passenger transportation and emergency cargo transportation immediately after the action of the L2 ground motion.
(2) Special seismic resistant quay walls (for main-line transportation): A facility which can be used for main-line transportation within a short period of time after the action of the L2 ground motion.
(3) Standard seismic resistant quay walls (for emergency transportation): A facility which can be used for mooring, passenger transportation and emergency cargo transportation within a certain period of time after the action of the L2 ground motion.

[Annex]

(1) Categorization of seismic resistant facilities[9]

Seismic resistant facilities can be categorized as Table 2 in terms of functions expected after the earthquake and the period in which the functions should be recovered.

Table 2 Categorization of seismic resistant facilities

	Seismic resistant facilities		
	Special		Standard
	for emergency transportation	for main-line transportation	for emergency transportation
Functions expected after the action of L2 ground motion	can be used for mooring, passenger transportation and emergency cargo transportation immediately after the action of the L2 ground motion	can be used for main-line transportation within a short period of time after the action of the L2 ground motion	can be used for mooring, passenger transportation and emergency cargo transportation within a certain period of time after the action of the L2 ground motion
	particular functions after the earthquake	ordinary functions	particular functions after the earthquake
Allowable amount of restoration work[10]	a slight restoration work	a slight restoration work	a limited amount of restoration work

[9] The term “seismic resistant facilities” refers to both “seismic resistant quay walls” and “seismic resistant pile-supported wharves”.
[10] This means the allowable amount of restoration work before temporary use after the earthquake.

3.1 General

[Notification] (Performance Criteria for Quay Walls for L2 Ground Motion)
Article 48
The extent of damage to seismic-resistant quay walls due to the L2 ground motion should be within a limit which is designated in accordance with the performance requirements.

[Commentary]
(1) Seismic-resistant quay wall of gravity type
a) Special seismic resistant quay wall (for emergency transportation) of gravity type
The limit of deformation of a special seismic resistant quay wall (for emergency transportation) of gravity type should be determined appropriately so that the quay wall can be used immediately after the earthquake for mooring and transportation of emergency goods, refugees and equipments for emergency construction. In general, the limit can be designated in terms of the residual horizontal displacement of the quay wall.
b) Special seismic resistant quay wall (for main-line transportation) of gravity type
The limit of deformation of a special seismic resistant quay wall (for main-line transportation) of gravity type should be determined appropriately so that the function of the quay wall can be recovered with only a slight restoration work after the earthquake. The deformation should be within the allowable deformation depending on the characteristics of the cargo handling machinery to be installed. In general, the limit can be designated in terms of the residual horizontal displacement of the quay wall, the tilt of the quay wall and the relative displacement of two rails of the cargo handling machinery.
c) Standard seismic resistant quay wall (for emergency transportation) of gravity type
The limit of deformation of a standard seismic resistant quay wall (for emergency transportation) of gravity type should be determined appropriately so that the quay wall can be used for transportation of emergency goods after a limited amount of restoration work after the earthquake. In general, the limit can be designated in terms of the residual horizontal displacement of the quay wall.
(2) Seismic-resistant quay wall of sheet-pile type
a) Special seismic resistant quay wall (for emergency transportation) of sheet-pile type
1) The limit of deformation of a special seismic resistant quay wall (for emergency transportation) of sheet-pile type should be determined in the same way as that of a special seismic resistant quay wall (for emergency transportation) of gravity type.
2) The stress in the sheet pile of a special seismic resistant quay wall (for emergency transportation) of sheet-pile type should not exceed the yield stress.
3) The stress in the tie rod of a special seismic resistant quay wall (for emergency transportation) of sheet-pile type should not exceed the tensile strength.
4) There are several types of anchors for sheet-pile quay walls. Appropriate quantities to be verified should be selected depending on the type the anchor. In the case of anchor pile, the moment in the anchor pile should not exceed the full plastic moment. In the case of coupled anchor piles, the tensile and compressional axial force in the anchor piles should not exceed the maximum resistance of the soil.
5) The stress acting in the upper structure should not exceed the strength of the material.
b) Special seismic resistant quay wall (for main-line transportation) of sheet-pile type
The performance criteria for a special seismic resistant quay wall (for main-line transportation) of sheet-pile type should be determined in the same way as those for a special seismic resistant quay wall (for emergency transportation) of sheet-pile type, except that the limit of deformation of a special seismic resistant quay wall (for mail-line transportation) of sheet-pile type should be determined in the same way as that of a special seismic resistant quay wall (for main-line transportation) of gravity type.
c) Standard seismic resistant quay wall (for emergency transportation) of sheet-pile type
1) The limit of deformation of a standard seismic resistant quay wall (for emergency transportation) of sheet-pile type should be determined in the same way as that of a standard seismic resistant quay wall (for emergency transportation) of gravity type.

2) The moment in the sheet pile of a standard seismic resistant quay wall (for emergency transportation) of sheet-pile type should not exceed the full plastic moment.
3) The stress in the tie rod of a standard seismic resistant quay wall (for emergency transportation) of sheet-pile type should not exceed the tensile strength.
4) There are several types of anchors for sheet-pile quay walls. Appropriate quantities to be verified should be selected depending on the type the anchor. In the case of anchor pile, the moment in the anchor pile should not exceed the full plastic moment. In the case of coupled anchor piles, the tensile and compressional axial force in the anchor piles should not exceed the maximum resistance of the soil.
5) The stress acting in the upper structure should not exceed the strength of the material.

3.2 Earthquake Resistant Design of Gravity Quay Walls

[Notification] (Performance Criteria for Gravity Quay Walls for L1 Ground Motion)
Article 49
For the L1 ground motion, the probability of failure should not exceed a prescribed value for three failure modes, namely, the sliding of the quay wall, the overturning of the quay wall and the lack of bearing capacity of the underlying ground.

[Commentary]
The failure of a gravity quay wall due to three modes can be regarded as equivalent to the occurrence of residual horizontal displacement of 10cm at the top of the quay wall.

[Annex]

(1) Outline of performance verification

A typical cross section of a gravity quay wall is shown in Figure 9. A recommended procedure for the performance verification of a gravity quay wall is shown in Figure 10. Performance verification for the L1 ground motion can be carried out with a pseudo static approach. Performance verification of seismic-resistant quay walls for the L2 ground motion should be carried out with a detailed dynamic analysis.

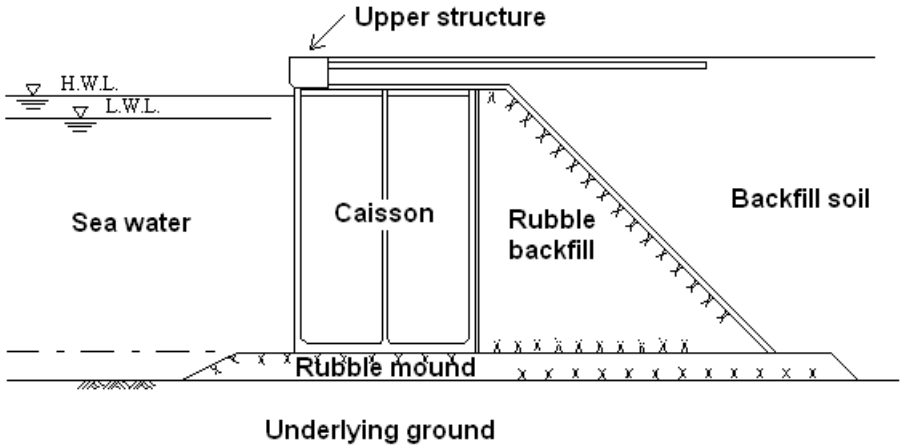

Figure 9 A typical cross section of a gravity quay wall.

It should be noted that the failure modes assumed in the pseudo-static approach such as sliding or overturning are not necessarily consistent with actual failure modes observed in the past case histories. For

example, field investigations at Kobe Port after the 1995 Hyogo-ken Nanbu earthquake (M7.3) revealed that, although the caisson quay walls exhibited several meters of horizontal displacement, no significant relative displacement was found between the caisson and the rubble mound, *i.e.*, the horizontal displacement of the caisson was mainly caused by the shear deformation of the rubble mound and/or the underlying ground (Inagaki *et al.*, 1996). This result of field investigation is consistent with the results of shake table tests and effective stress analysis (Inagaki *et al.*, 1996). Taking these observations into account, the pseudo static approach described in (2) is designed to determine a cross section of a gravity quay wall which satisfies the criteria in terms of horizontal displacement (typically 10cm)[11]. The approach in (2) is based on the assumptions that the displacement of the quay wall is induced by the deformation of the rubble mound and/or the underlying ground. Therefore, in the case of a caisson directly put on a firm ground, it is recommended to use sliding block analysis, etc. instead of relying on the procedure described in (2).

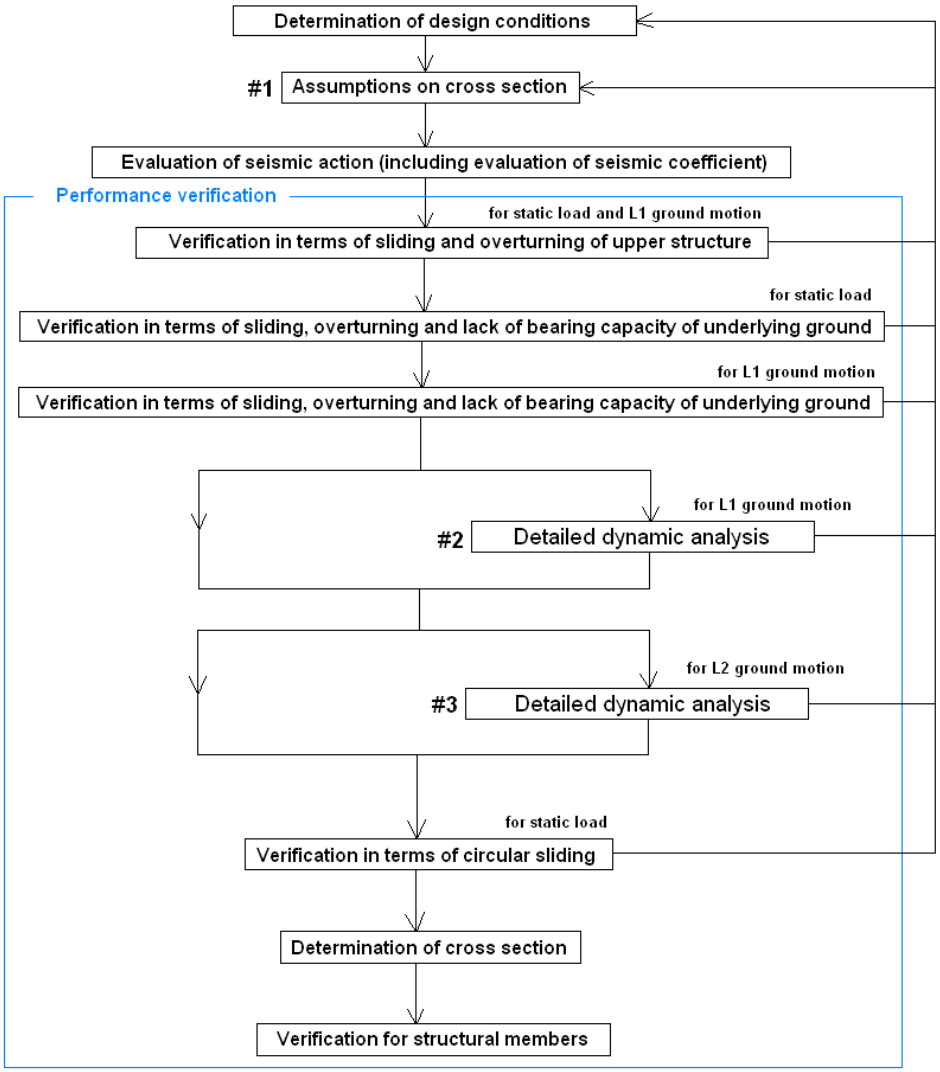

#1 In assuming the cross section, effect of liquefaction should be considered.
#2 For the L1 ground motion, dynamic analysis should be cariied out to evaluate residual deformation when necessary.
#3 For the L2 ground motion, dynamic analysis should be carried out to evaluate residual deformation for seismic resistant quay walls.

Figure 10 Procedure for the performance verification of a gravity quay wall.

[11] It was confirmed by dynamic FEM analyses that the cross section determined through the pseudo static approach in (2) satisfies the criteria in terms of horizontal displacement.

(2) Performance verification with pseudo static approach

The pseudo static approach described in this section is based on the assumptions that the effect of excess pore water pressure on the performance of the quay wall is negligible. Therefore, before using this approach, the engineers should make sure that the effect of excess pore water pressure is negligible. If liquefiable soil is found around the structure, appropriate liquefaction countermeasures should be taken.

The procedure for evaluating the seismic coefficient can be described as Figure 11. First, 1D earthquake response analysis of ground should be carried out, using the L1 ground motion at the outcrop of a firm ground, to evaluate the acceleration time history at the ground surface. Then, the acceleration Fourier spectrum at the ground surface is calculated and it is filtered with a structure-type dependent filter to omit high frequency contents which are less important for the deformation of gravity quay walls. The filtered spectrum is transformed back into time domain to obtain another acceleration time history. The peak value of the acceleration time history after filtering is defined as α_f. Thirdly, α_f is multiplied by a factor of correction p to obtain α_c. Finally, from α_c and the allowable displacement D_a, the seismic coefficient can be evaluated.

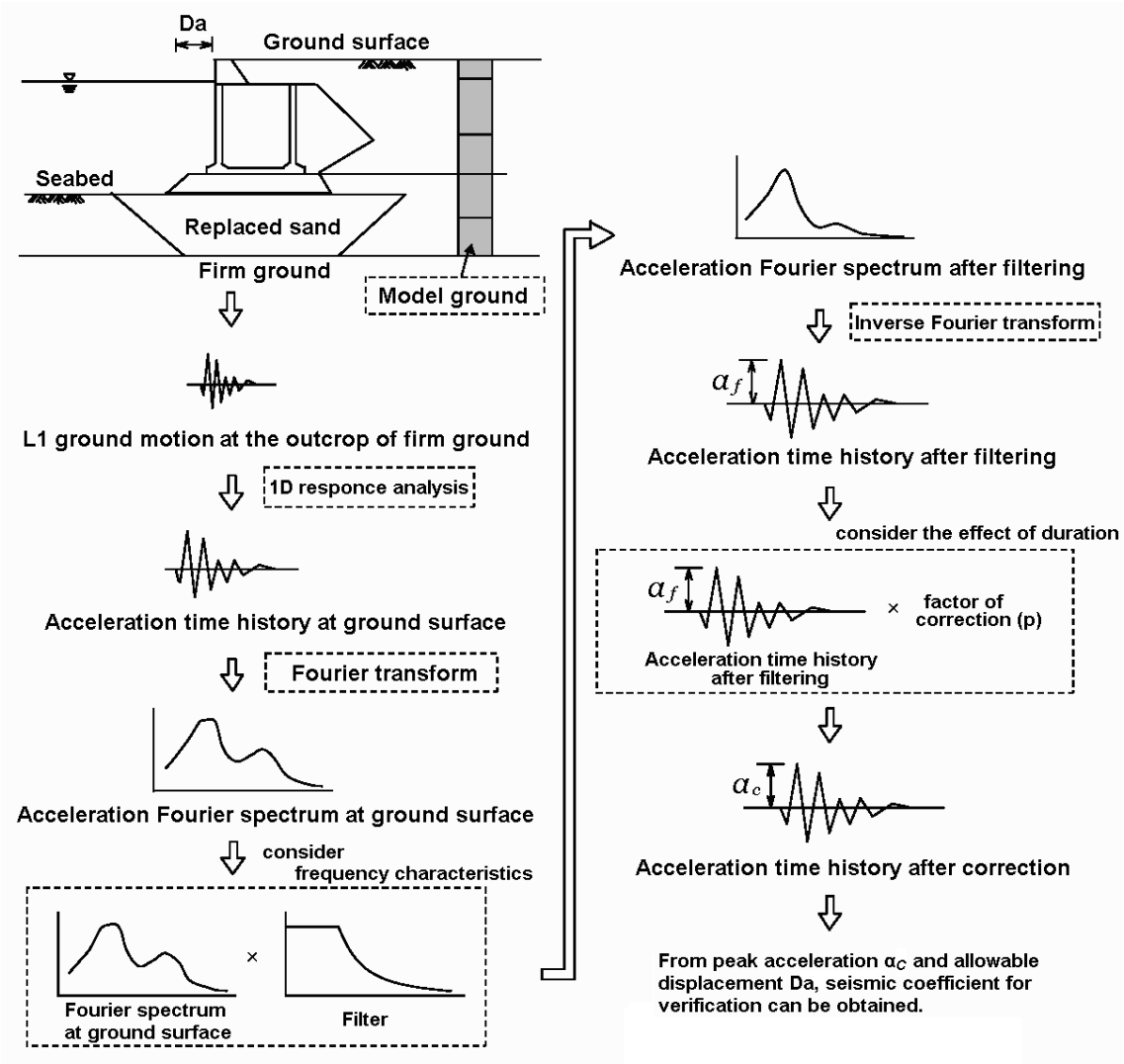

Figure 11 Procedure for the evaluation of seismic coefficient.

In the case of a gravity quay wall, the filter in equation (17) can be used.

$$a(f) = \begin{cases} b & 0 < f \le 1.0 \\ \dfrac{b}{1 - \left(\dfrac{f - 1.0}{1/0.34}\right)^2 + 6.8\left(\dfrac{f - 1.0}{1/0.34}\right)\mathrm{i}} & 1.0 \le f \end{cases} \tag{17}$$

$$b = 1.05\frac{H}{H_R} - 0.88\frac{T_b}{T_{b_R}} + 0.96\frac{T_u}{T_{u_R}} - 0.23\ ,$$

where

a: the filter for a gravity quay wall
f: frequency (Hz)
H: wall height (m)
H_R: wall height for reference (=15 m)
T_b: initial natural period of backfill soil (s)
T_{bR}: initial natural period of backfill soil for reference (=0.8 s)
T_u: initial natural period of underlying ground (s)
T_{uR}: initial natural period of underlying ground for reference (=0.4 s)
i: imaginary unit

The value *b* should be determined to satisfy following two conditions.

$$0.04\ H + 0.08 \le b \le 0.04\ H + 0.44 \tag{18}$$

$$b \ge 0.28 \tag{19}$$

In the above, T_u and T_b should be calculated from the soil columns designated in Figure 12.

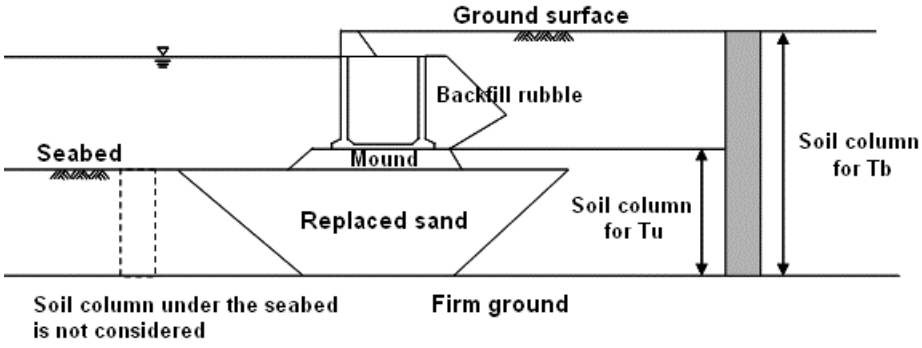

Figure 12 Soil columns from which T_u and T_b should be calculated.

An example of the filter is shown in Figure 13.

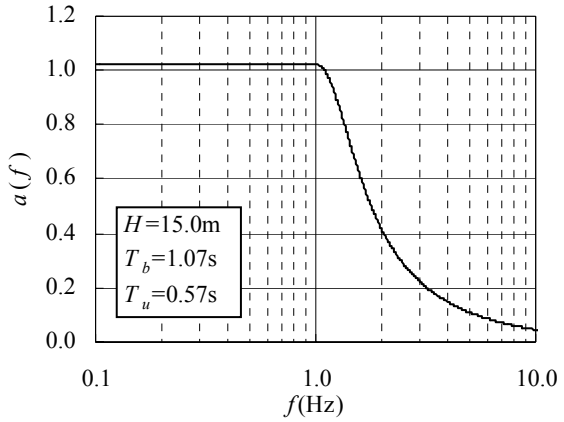

Figure 13 Example of the filter for a gravity quay wall.

The factor of correction *p* can be obtained as

$$p = 0.36 \ln\left(S / a_f\right) - 0.29 \tag{20}$$

In the equation (20), it is understood that *p* does not exceed 1.0. In the equation (20), *S* is the root of the sum of the squared acceleration, defined as

$$S = \sqrt{\sum acc^2} \quad , \tag{21}$$

where *acc* is the acceleration time history after filtering (sampling frequency is assumed to be 100Hz). Finally, the characteristic value of the seismic coefficient can be obtained from α_c and the allowable displacement D_a as

$$k_{hk} = 1.78 \left(\frac{D_a}{D_r}\right)^{-0.55} \frac{\alpha_c}{g} + 0.04 \qquad (5\text{cm} < D_a < 20\text{cm}) \tag{22}$$

where k_{hk} is the characteristic value of the seismic coefficient, D_a is the allowable horizontal residual displacement at the top of the quay wall (typically 10cm) and D_r is a reference displacement (10cm). The equation (22) is valid for 5cm< D_a <20cm. In the equation (22) it is understood that k_{hk} is in the range from 0.05 – 0.25.

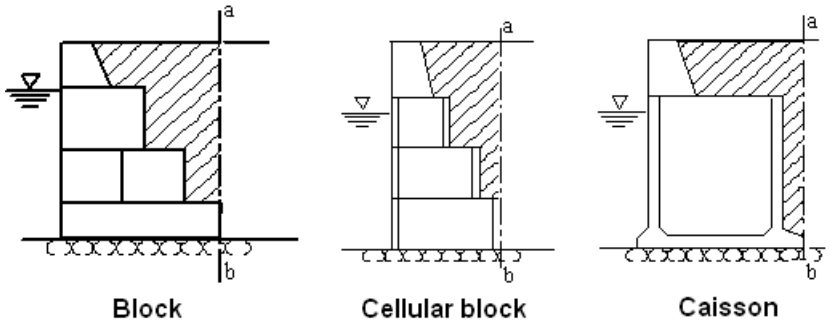

Figure 14 Definition of the “wall” for pseudo static approach.

In the performance verification for a gravity quay wall, hatched portion in Figure 14 can be regarded as a

part of the wall.

(a) Sliding of wall

The following inequality can be used for the performance verification in terms of the sliding of the wall[12].

$$f_d\left(W_d + P_{Vd} - P_{Bd}\right) \geq \gamma_a\left(P_{Hd} + P_{wd} + P_{d_{wd}} + P_{Fd}\right), \tag{23}$$

where

f: friction coefficient
W: weight of the wall
P_V: vertical earth pressure resultant acting on the wall
P_B: buoyancy acting on the wall
P_H: horizontal earth pressure resultant acting on the wall
P_W: residual water pressure resultant acting on the wall
P_{dW}: hydrodynamic pressure resultant acting on the wall
P_F: inertia force acting on the wall
γ_a: structural analysis factor (=1.0)

The design values can be obtained from the characteristic values using the following equations.

$$\begin{aligned} f_d &= \gamma_f f_k \\ P_{Hd} &= \gamma_{P_H} P_{Hk} \\ P_{Vd} &= \gamma_{P_V} P_{Vk} \\ P_{d_{wd}} &= \frac{7}{12}\gamma_{k_h} k_{hk} \rho_w g h^2 \\ P_{Fd} &= \gamma_{k_h} k_{hk} W_d \end{aligned} \quad , \tag{24}$$

where

ρ_w: density of sea water
g: acceleration of gravity
h: water depth in front of the wall
k_h: seismic coefficient for verification

To calculate the characteristic value of the earth pressure, the Mononobe-Okabe method (*e.g.*, the International Organization for Standardization, 2005) can be used. To calculate the characteristic value of the earth pressure, the characteristic value of the residual water level should be used. The design value of the residual water pressure should be calculated from the design value of the residual water level. The design value of the residual water level can be obtained from the characteristic value of the residual water level as follows.

$$RWL_d = \gamma_{RWL} RWL_k \tag{25}$$

The design value of the weight of the wall can be obtained from the characteristic value of the weight of the wall as follows.

[12] Throughout this article, the subscripts *k* and *d* indicate the characteristic value and the design value, respectively. In addition, γ indicates the partial factor corresponding to the quantity indicated by the subscript.

$$W_d = \gamma_W W_k \tag{26}$$

As for the partial factors appearing in the equations above, 1.0 can be used as long as the L1 ground motion is concerned.

(b) Bearing capacity of underlying ground

The performance verification in terms of the bearing capacity of the underlying ground can be based on the simplified Bishop method[13] shown in Figure 17, based on the following equation.

$$\gamma_{F_f} F_f = \frac{\sum \left\{ [c_d s + (w'_d + q_d) \tan \phi_d] \dfrac{\sec \theta}{1 + \tan \theta \tan \phi_d / \left(\gamma_{F_f} F_f\right)} \right\}}{\sum \left\{ \left(w'_d + q_d\right) \sin \theta + a \, P_{H_d} / R \right\}} \tag{27}$$

where

R: radius of the circular failure surface
θ : angle between the horizontal plane and the failure surface at the soil column
s: width of the soil column
w': effective weight of the soil column for unit length (with considerations of buoyancy)
q: vertical load from the wall acting on the soil column for unit length
P_H: total horizontal load from the wall for unit length

[13] The equation (27) can be obtained as follows. Let *T* denote the friction acting at the bottom of the soil column for unit length. If we consider the overall balance of the moments for the circle shown in Figure 17, we obtain

$$\frac{R \sum T}{\sum \left\{ \left(w' + q\right) R \sin \theta + a \, P_H \right\}} > 1$$

which is equivalent to

$$\frac{\sum T}{\sum \left\{ \left(w' + q\right) \sin \theta + a \, P_H / R \right\}} > 1 \tag{7.1}$$

On the other hand, if we consider the balance of the vertical forces for the triangle shown in the right of Figure 17, we obtain

$$\begin{aligned} \sigma_v' &= \tau \tan\theta + \sigma_n' \\ \sigma_v' &= \left(w' + q\right) / s \\ \tau &= T / \left(s \sec \theta\right) \end{aligned} \tag{7.2}$$

Furthermore, if we consider the fact that the bottom plane of the soil column satisfies the failure criteria, we obtain

$$\sigma_n' = \frac{\tau - c}{\tan \phi} \tag{7.3}$$

By substituting equations (7.2) and (7.3) into (7.1), one can obtain the equation (27).

a: distance shown in Figure 15
c: cohesion of the material
ϕ_d: internal friction angle of the material

From the equation (27), the value *F* can be obtained. If *F*>1, the bearing capacity is sufficient.

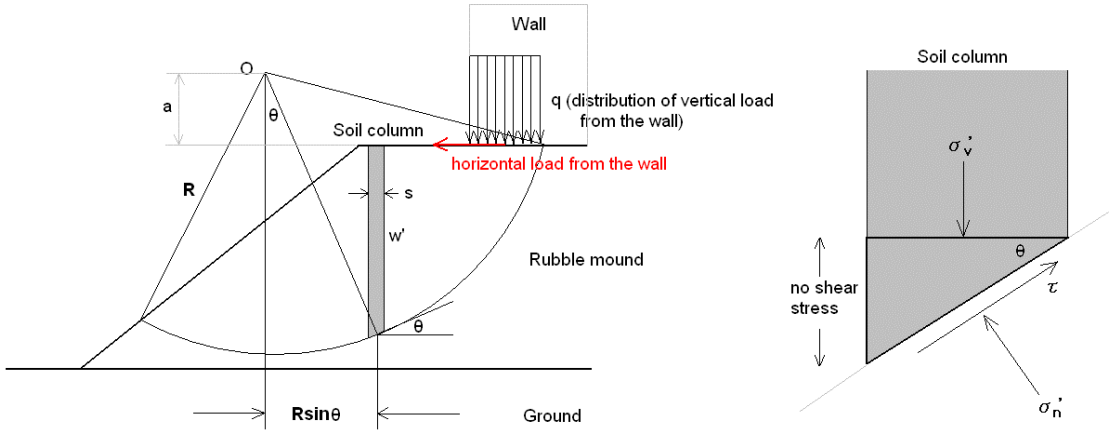

Figure 15 Schematic diagram showing the simplified Bishop method.

The design values can be obtained from the characteristic values using the following equations.

$$
\begin{aligned}
c_d &= \gamma_c c_k \\
\tan\phi_d &= \gamma_{\tan\phi} \tan\phi_k \\
w'_d &= \gamma_{w'} w'_k \\
q_d &= \gamma_q q_k \\
P_{Hd} &= \gamma_{P_H} P_{Hk}
\end{aligned}
\tag{28}
$$

As shown in Figure 15, the vertical load from the wall should be approximated as a uniformly distributed load beginning from one corner of the wall, taking into account the point of application. Then a failure surface starting from the end point of the distributed load should be considered. It is not necessary to consider horizontal inertia force acting on the rubble mound and the ground. As for the cohesion and the internal friction angle of the rubble mound, c=20kN/m^2 and ϕ_d=35° can be used, respectively (Kobayashi *et al*., 1987), as long as the compressive strength of the parent rock is larger than 30MN/m^2. If the compressive strength of the parent rock is smaller than 30MN/m^2, c=20kN/m^2 and ϕ_d=30° can be used (Mizukami and Kobayashi, 1991). For sandy soil with the SPT N value less than 10, ϕ_d=40° can be used. For sandy soil with the SPT N value larger than 10, ϕ_d=45° can be used. The applicability of the method described above has been revealed from model tests, field tests and analyses of existing breakwaters and quay walls (Kobayashi *et al*., 1987).

As for the partial factors appearing in the equations above, 1.0 can be used as long as the L1 ground motion is concerned.

(c) Overturning of wall

The following inequality can be used for the performance verification in terms of the overturning of the wall.

$$
a\, W_d - b\, P_{Bd} + c\, P_{Vd} \geq \gamma_a \left(d\, P_{Hd} + e\, P_{wd} + h\, P_{d_{wd}} + i\, P_{Fd} \right), \tag{29}
$$

where

a: distance between the wall front and the application point of the weight of the wall
b: distance between the wall front and the application point of the buoyancy acting on the wall
c: distance between the wall front and the application point of the vertical earth pressure resultant acting on the wall
d: distance between the bottom of the wall and the application point of the horizontal earth pressure resultant acting on the wall
e: distance between the bottom of the wall and the application point of the residual water pressure resultant acting on the wall
f: distance between the bottom of the wall and the application point of the hydrodynamic pressure resultant acting on the wall
g: distance between the bottom of the wall and the application point of the inertia force acting on the wall
γ_a: structural analysis factor (=1.1)

As for the partial factors appearing in the equations above, 1.0 can be used as long as the L1 ground motion is concerned.

(3) Performance verification with detailed dynamic analysis

The performance of seismic-resistant quay walls of gravity type for the L2 ground motion is most typically evaluated with a two-dimensional effective-stress finite element analysis.

In the performance verification of port facilities, the decrease of effective stress in the ground due to the excess pore water pressure is not negligible in many cases. The decrease of effective stress leads to a change in the stress-strain relation and the damping characteristics of the soil. To take into account these effects appropriately, effective stress analyses are required.

The stress-strain relation of the soil is specified by constitutive models. The existing constitutive models fall into three categories, namely, the linear model, the equivalent-linear model and the nonlinear model. To evaluate the residual deformation of a quay wall as shown in Figure 16, it is necessary to employ a nonlinear constitutive model.

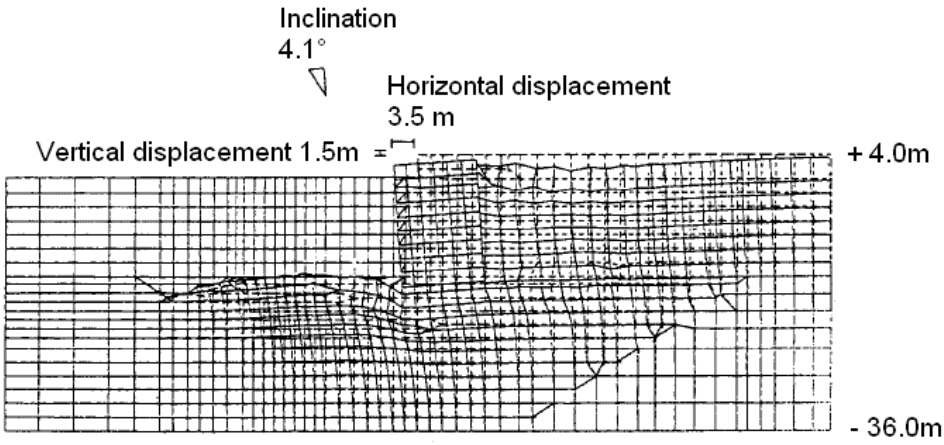

Figure 16 Residual deformation of a quay wall evaluated by the effective stress analysis

The computer program FLIP (Iai *et al*., 1992) is one of the most frequently used programs for the two-dimensional effective-stress finite element analysis. Its applicability for port facilities has been

demonstrated through the analysis of case histories (Ichii *et al.*, 1997; Iai *et al.*, 1998).

Some of the important issues related to the reliability of the analytical results can be summarized as follows.

It is obviously necessary to employ a program whose applicability has been demonstrated through the analysis of case histories. In addition, computer programs for the effective stress analysis are undergoing continuous improvement. Sometimes one computer program supports different (old and new) algorithms. Therefore, it is not enough to pay attention to the name of the program. It is necessary to make sure that the program is used in the same way as it was used for the case history analysis. It is strongly recommended to keep the whole input data used for the analysis.

A sufficiently large analytical domain should be prepared. It is recommended that the analytical domain extends down to the upper boundary of the firm ground, because the design ground motions are specified at the outcrop of the firm ground. A viscous boundary should be implemented at the bottom of the model. It is important to make sure that the shear wave velocity of the firm ground assumed in the determination of design ground motions and that assumed in the effective stress analysis are in agreement. In general, in-plane horizontal ground motions are required for the two dimensional analysis. The in-plane horizontal ground motions can be obtained from two horizontal components.

The side boundaries of the analytical domain should be sufficiently away from the wall. Judging from the case history during the 1995 Hyogo-ken Nanbu earthquake, the landward side boundary should be at least 100 m away from the wall.

The mesh size should be determined taking into account the length of the waves to be considered. The mesh size should be at least as small as 1/5 the wavelength to be considered. The decrease of the wavelength due to liquefaction should also be considered. In this case, the shear modulus after liquefaction is assumed to be 1/50 the shear modulus for small strains in practice.

In principle, the material parameters should be determined based on geotechnical investigations. Preferable investigations can be summarized as follows.

- PS logging is required to determine the shear wave velocity and, consequently, the shear modulus of the soil.
- For sandy soil, the liquefaction resistance should be evaluated by a cyclic triaxial test or a cyclic torsional test on undisturbed samples. In the tests, it is important to obtain not only the liquefaction resistance but also the time history of excess pore water and shear strain, because these time history data provide important constraints on the material parameters.
- It is preferable to conduct standard penetration tests even when cyclic triaxial or torsional test data are available because the internal friction angle of a sandy soil is often evaluated from the SPT N value. The shear modulus of a thin layer is often evaluated from the SPT N value.
- For cohesive soil, the compressive strength should be evaluated by a laboratory test. The result can be used to evaluate the shear modulus and the shear strength of the soil.

Parameters for damping including the coefficient for Rayleigh damping should be determined appropriately. It is preferable to employ parameters which are consistent with past case histories.

Care should be taken when the results of the effective-stress finite element analysis are compared with the performance criteria. For example, for the quay wall to be used immediately after the earthquake for the transportation of emergency goods, etc., the relative vertical displacement between the wall and the backfill should be small enough. The numerical result for the relative vertical displacement between the wall and the backfill, however, is not as accurate as that for other quantities such as the overall horizontal displacement of the wall. On the other hand, for the quay wall to be used immediately after the earthquake for mooring, the variation of the horizontal displacement of the wall should be small enough. It is difficult,

however, to evaluate the variation of the horizontal displacement numerically. In this case it is more reasonable to evaluate the variation empirically, based on the numerically-evaluated overall horizontal displacement of the wall

3.3 Earthquake Resistant Design of Sheet-Pile Quay Walls[14]

[Notification] (Performance Criteria for Sheet-pile Quay Walls for L1 Ground Motion)
Article 50
(1) For the L1 ground motion, the sheet pile should be sufficiently stable (with sufficiently long embedded portion) and the probability of the stress in the sheet pile exceeding the yield stress should not exceed a prescribed value.
(2) For the L1 ground motion, the location of the anchor should be appropriate and the probability of the stability of the anchor being lost should not exceed a prescribed value.
(3) For the L1 ground motion, the probability of the stress in the tie rod exceeding the yield stress should not exceed a prescribed value.
(4) For the L1 ground motion, the probability of the stress in the upper structure exceeding the strength of the material should not exceed a prescribed value.

[Commentary]
(1) If the residual horizontal displacement at the top of the quay wall is less than 15cm, then both the sheet pile and the anchor can be considered sufficiently stable.
(2) In the case of anchor pile, the probability of the stress in the anchor pile exceeding the yield stress should not exceed a prescribed value. In the case of coupled anchor piles, the probability of the tensile and compressional axial force in the anchor piles exceeding the maximum resistance of the soil should not exceed a prescribed value.
(3) If the connecting elements are special or large, appropriate performance criteria should be established in terms of the stress in the connecting elements.

[Annex]

(1) Outline of performance verification

A typical cross section of an anchored sheet-pile quay wall is shown in Figure 17. A recommended procedure for the performance verification of a sheet-pile quay wall is shown in Figure 18. Performance verification for the L1 ground motion can be carried out with a pseudo static approach. Performance verification of seismic-resistant quay walls for the L2 ground motion should be carried out with a detailed dynamic analysis.

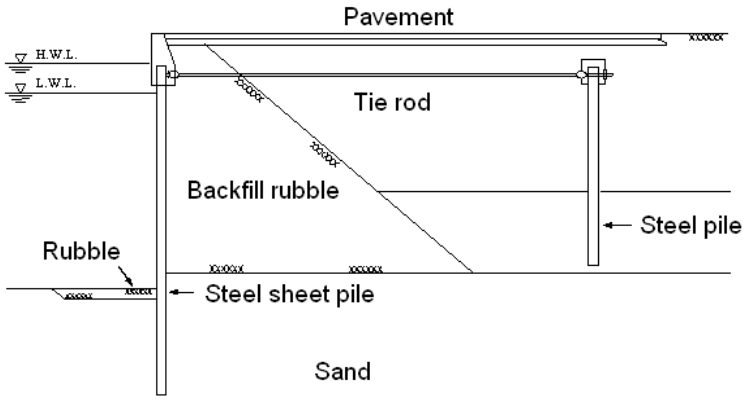

Figure 17 A typical cross section of an anchored sheet-pile quay wall.

[14] In this section, it is assumed that the sheet-pile quay wall has an anchor.

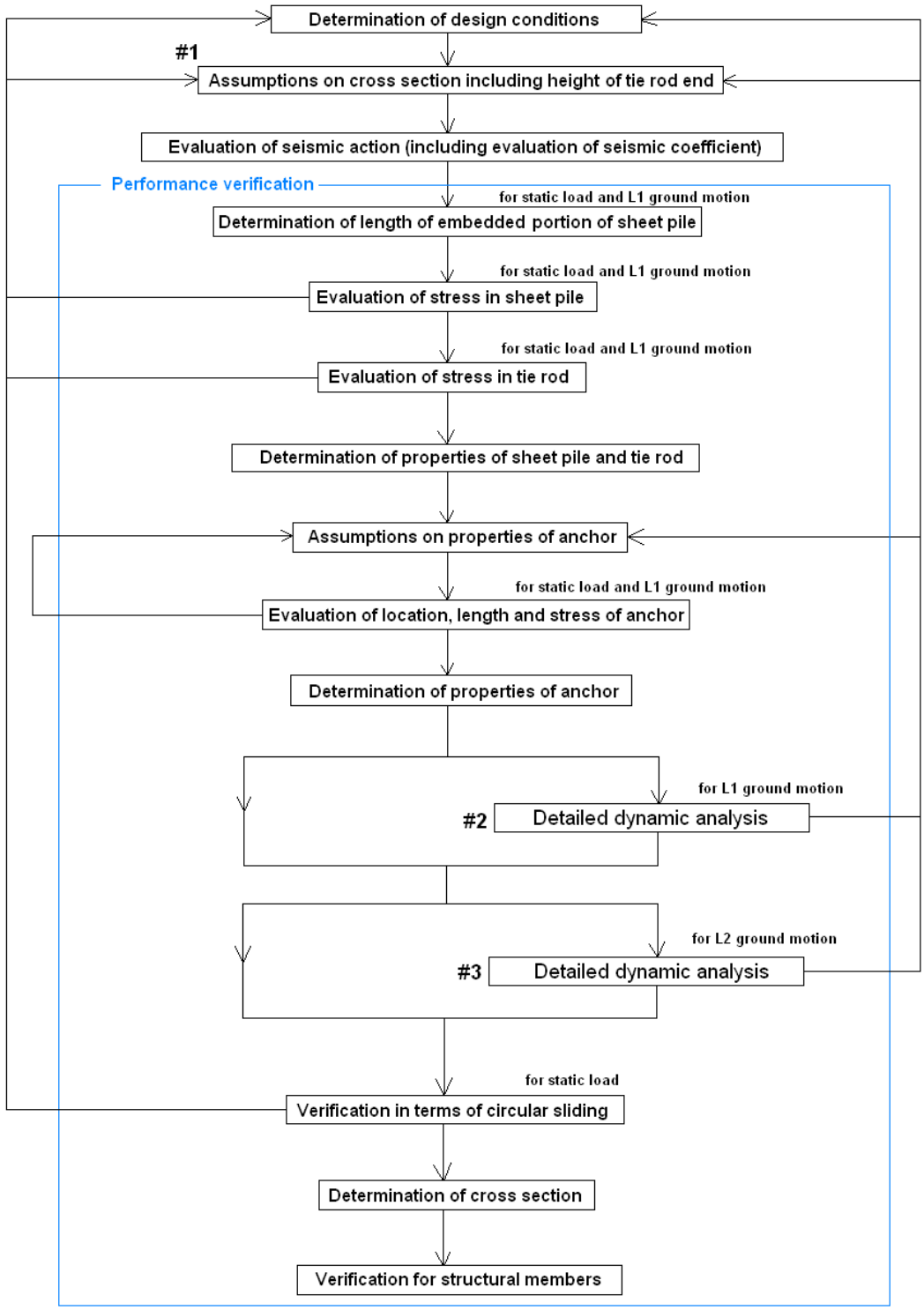

#1 In assuming the cross section, effect of liquefaction should be considered.
#2 For the L1 ground motion, dynamic analysis should be cariied out to evaluate residual deformation when necessary.
#3 For the L2 ground motion, dynamic analysis should be carried out to evaluate residual deformation for seismic resistant quay walls.

Figure 18 Procedure for the performance verification of a sheet-pile quay wall.

(2) Performance verification with pseudo static approach

The pseudo static approach described in this section is designed to determine a cross section of a sheet-pile quay wall which satisfies the criteria in terms of horizontal displacement (typically 15cm)[15].

The pseudo static approach described in this section is based on the assumptions that the effect of excess pore water pressure on the performance of the quay wall is negligible. Therefore, before using this approach, the engineers should make sure that the effect of excess pore water pressure is negligible. If liquefiable soil is found around the structure, appropriate liquefaction countermeasures should be taken.

The procedure for evaluating the seismic coefficient for a sheet-pile quay wall is similar to that for a gravity quay wall (Figure 11). It should be noted, however, that the filter, the factor of correction *p* and the equation to determine the seismic coefficient are different from those for a gravity quay wall.

In the case of a sheet-pile quay wall with anchor piles, the filter in equation (30) can be used.

$$a(f) = \begin{cases} b & 0 < f \le 1.0 \\ \dfrac{b}{1 - \left(\dfrac{f - 1.0}{1/0.34}\right)^2 + 11.0\left(\dfrac{f - 1.0}{1/0.34}\right)\mathrm{i}} & 1.0 \le f \end{cases} \tag{30}$$

$$b = 2.25\frac{H}{H_R} - 0.88\frac{T_b}{T_{bR}} + 0.96\frac{T_u}{T_{uR}} - 0.96 \quad \text{(with vertical anchor piles)}$$

$$b = 2.25\frac{H}{H_R} - 0.88\frac{T_b}{T_{bR}} + 0.96\frac{T_u}{T_{uR}} - 0.76 \quad \text{(with coupled anchor piles)}$$

where

a: the filter for a sheet-pile quay wall with anchor piles
f: frequency (Hz)
H: wall height (m)
H_R: wall height for reference (=15 m)
T_b: initial natural period of backfill soil (s)
T_{bR}: initial natural period of backfill soil for reference (=0.8 s)
T_u: initial natural period of underlying ground (s)
T_{uR}: initial natural period of underlying ground for reference (=0.4 s)
i: imaginary unit

The value *b* should be determined to satisfy following conditions.

$$0.12\,H + 0.78 \le b \le 0.12\,H + 0.24 \quad \text{(with vertical anchor piles)}$$

$$0.12\,H + 0.78 \le b \le 0.12\,H + 0.04 \quad \text{(with coupled anchor piles)} \tag{31}$$

$$b \ge 0.41$$

[15] It was confirmed by dynamic FEM analyses that the cross section determined through the pseudo static approach described in this section satisfies the criteria in terms of horizontal displacement.

In the above, T_u and T_b should be calculated from the soil columns designated in Figure 19.

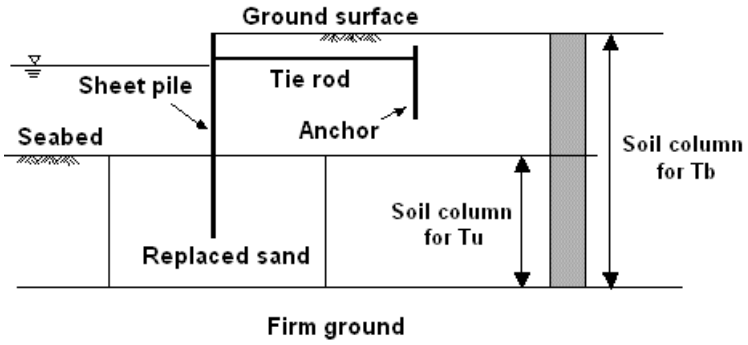

Figure 19 Soil columns from which T_u and T_b should be calculated.

Examples of the filter for sheet-pile quay walls with vertical anchor piles and coupled anchor piles are shown in Figure 20.

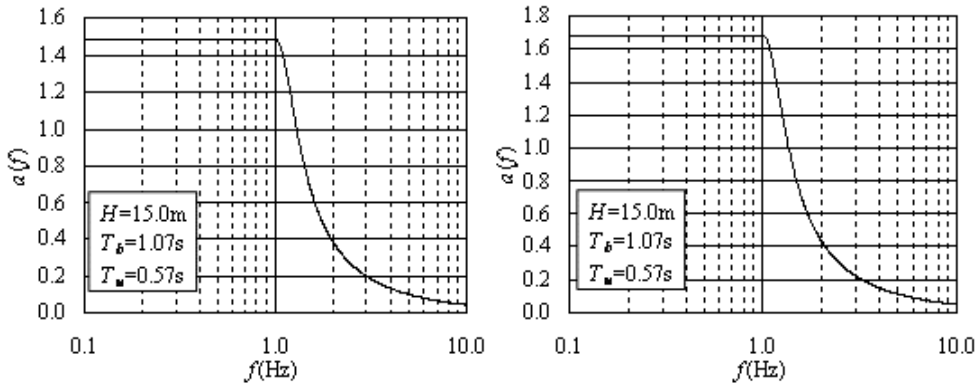

Figure 20 Examples of the filter for sheet-pile quay walls with vertical anchor piles (left) and coupled anchor piles (right).

The factor of correction p can be obtained as

$$p = 0.35 \ln\left(S / a_f\right) - 0.20 \quad \text{(with vertical anchor piles)}$$
$$p = 0.31 \ln\left(S / a_f\right) - 0.10 \quad \text{(with coupled anchor piles)} \qquad (32)$$

In the equation (32), it is understood that p does not exceed 1.0. In the equation (32), S is the root of the sum of the squared acceleration, defined as

$$S = \sqrt{\sum acc^2} \qquad (33)$$

where acc is the acceleration time history after filtering (sampling frequency is assumed to be 100Hz). Finally, the characteristic value of the seismic coefficient can be obtained from α_c and the allowable displacement D_a as

$$k_{hk} = 1.91 \left(\frac{D_a}{D_r} \right)^{-0.69} \frac{\alpha_c}{g} + 0.03 \quad \text{(with vertical anchor piles) (5cm< } D_a \text{ <20cm)}$$

$$k_{hk} = 1.32 \left(\frac{D_a}{D_r} \right)^{-0.74} \frac{\alpha_c}{g} + 0.05 \quad \text{(with coupled anchor piles) (5cm< } D_a \text{ <20cm)} \qquad (34)$$

where k_{hk} is the characteristic value of the seismic coefficient, D_a is the allowable horizontal residual displacement at the top of the quay wall (typically 15cm) and D_r is a reference displacement (10cm). The equation (34) is valid for 5cm< D_a <20cm. In equation (34) it is understood that k_{hk} is in the range from 0.05 – 0.25.

The characteristic value of the seismic coefficient for a sheet-pile quay wall with vertical anchor piles can be applied to that with anchor sheet-piles or anchor plates.

(a) Length of embedded portion of sheet pile

The length of the embedded portion of the sheet pile can be determined as follows (Takahashi *et al*., 1993).

$$\frac{D_F}{H_T} \geq 5.0916\ \omega^{-0.2} - 0.2591$$

$$\omega = \rho\ l_h \qquad (35)$$

$$\rho = H_T^{\,4} / EI$$

where

D_F: length of the embedded portion of the sheet pile
H_T: height of the point fixed to the tie rod measured from the seabed
EI: flexural rigidity of the sheet pile
l_h: coefficient of subgrade reaction of the sheet pile.

In principle, the coefficient of subgrade reaction should be determined based on in-situ load tests. When load test data is not available, Figure 21 can be used to estimate the coefficient.

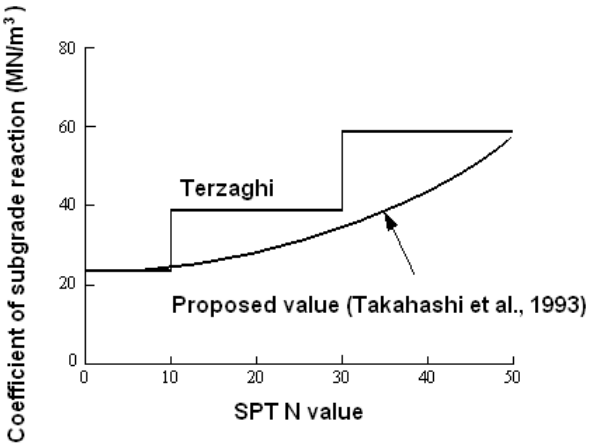

Figure 21 Relation between the SPT N value and the coefficient of subgrade reaction.

(b) Tension of tie rod and moment of sheet pile

The evaluation of the tension of the tie rod and the moment of the sheet pile can start from the virtual beam method. Figure 22 shows the assumptions made in the virtual beam method. A simple beam supported at the height of the tie rod and at the seabed is assumed, *i.e.*, the moment of the sheet pile is assumed to be zero at the seabed. This assumption, however, is apparently not realistic especially for sheet piles with high rigidity. Therefore, the results of the virtual beam method should be corrected later to take into account the effect of the rigidity of the wall appropriately.

In the virtual beam method, the reaction force due to the tie rod can be obtained from the following equation.

$$A_{pd} = P_{ad} + P_{wd} + P_{d_{wd}} - \frac{\left(a\,P_{ad} + b\,P_{wd} + c\,P_{d_{wd}}\right)}{L} \tag{36}$$

where

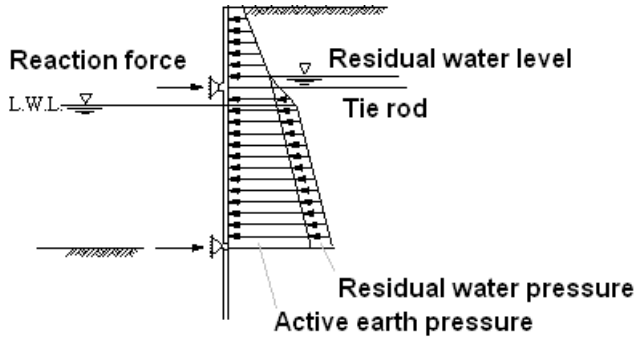

Figure 22 Assumptions for the virtual beam method

A_p: reaction force due to the tie rod
P_a: active earth pressure resultant acting on the wall
P_W: residual water pressure resultant acting on the wall
P_{dW}: hydrodynamic pressure resultant acting on the wall
a-*c*: distance from the point of application of each load to the point fixed to the tie rod
L: height of the point fixed to the tie rod measured from the seabed

To calculate the design value of the earth pressure, the Mononobe-Okabe method (*e.g.*, the International Organization for Standardization, 2005) can be used. To calculate the design value of the earth pressure, besides the design value of the seismic coefficient k_{hd}, the design value of the tangent of the internal friction angle tan ϕ_d, the design value of the cohesion c_d, the design value of the wall friction angle δ_d, the design value of the effective unit weight w'_d, the design value of the surcharge q_d, and the design value of the residual water level RWL_d should be considered. These design values can be determined from the characteristic values as

$$
\begin{aligned}
&\tan\phi_d = \gamma_{\tan\phi}\tan\phi_k \\
&c_d = \gamma_c c_k \\
&\delta_d = \gamma_\delta \delta_k \\
&w'_d = \gamma_{w'} w'_k \\
&q_d = \gamma_q q_k \\
&RWL_d = \gamma_{RWL} RWL_k
\end{aligned}
\tag{37}
$$

The design value of the residual water pressure can be obtained from the design value of the residual water level. The design value of the hydrodynamic pressure can be obtained from the following equation.

$$
P_{d_{wd}} = \frac{7}{12}\gamma_{k_h} k_{hk} \rho_w g h^2 \tag{38}
$$

The maximum moment of the sheet pile can be obtained from the following equation.

$$
M_{\max d} = a\, A_{pd} - b\, P'_{ad} - c\, P'_{wd} - d\, P'_{d_{wd}} \tag{39}
$$

where

M_{max}: maximum moment of the sheet pile
A_p: reaction force due to the tie rod
P_a': active earth pressure resultant above the point with zero shear force
P_W': residual water pressure resultant above the point with zero shear force
P_{dW}': hydrodynamic pressure resultant above the point with zero shear force
a: height of the point fixed to the tie rod measured from the point with zero shear force
b-d: distance from the point of application of each load to the point with zero shear force

Then, the design value of the reaction force due to the tie rod and the design value of the maximum moment of the sheet pile should be corrected by using the correction factors shown in Figures 23 and 24, respectively. As shown in Figures 23 and 24, the correction factors are the functions of ω defined in the equation (35).

The verification in terms of the moment of the sheet pile can be based on the following inequality in the case of steel sheet pile.

$$
\sigma_{yd} \geq \gamma_a \frac{M_{\max d}}{Z} \tag{40}
$$

where

σ_y: yield stress of the steel
M_{max}: maximum moment of the sheet pile
Z: section modulus of the sheet pile
γ_a: structural analysis factor (=1.12)

The design value of the yield stress of the steel can be obtained from the characteristic value as follows.

$$
\sigma_{yd} = \gamma_{\sigma_y} \sigma_{yk} \tag{41}
$$

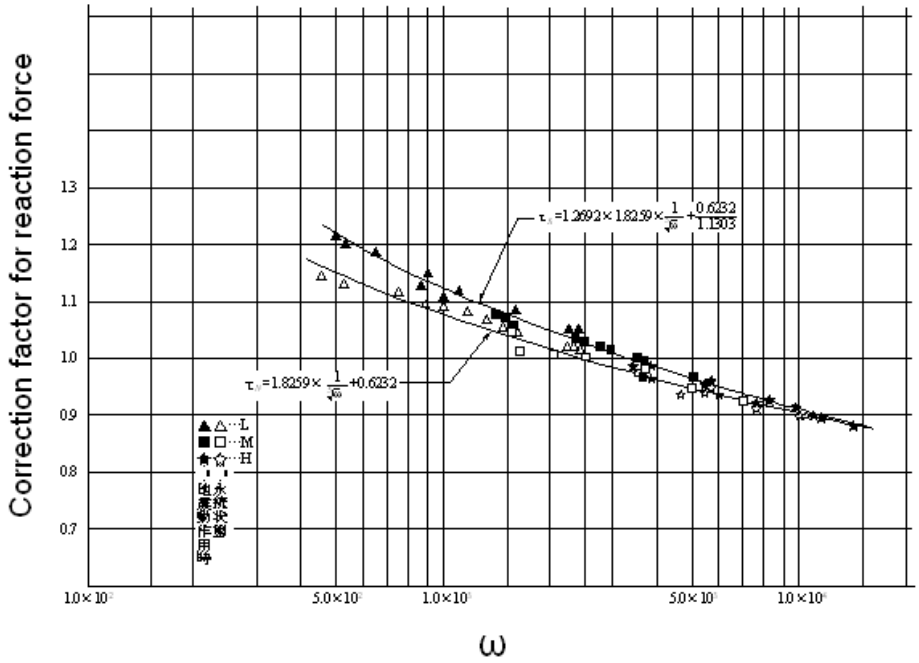

Figure 23 Correction factor for the reaction force

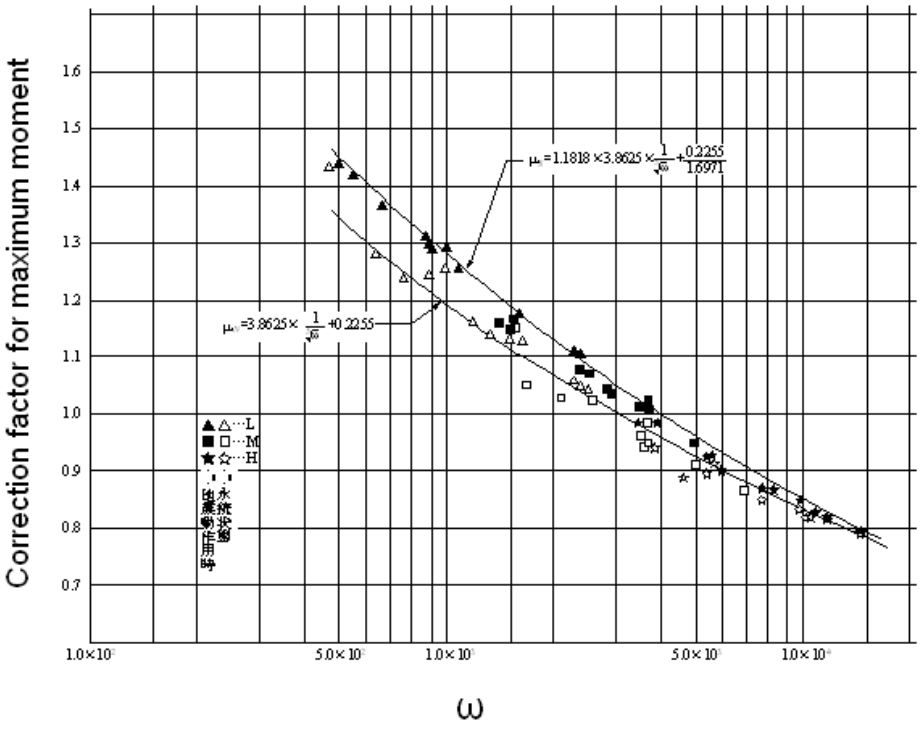

Figure 24 Correction factor for the maximum moment

The verification in terms of the tension of the tie rod can be based on the following inequality.

$$\sigma_{yd} \geq \gamma_a \frac{T_d}{A} \tag{42}$$

where

σ_y: yield stress of the steel
T_d: tension of the tie rod
A: cross-sectional area of the tie rod
γ_a: structural analysis factor (=1.67)

The tension of the tie rod can be obtained from the reaction force based on the following equation, taking into account the fact that the reaction force appearing in the equation (36) is for the unit length and that the tie rod might not be necessarily perpendicular to the coastline.

$$T_d = A_{pd}\, l \sec\theta \tag{43}$$

where l is the interval of the tie rod along the coastline and θ is the angle between the tie rod and the line perpendicular to the coast line.

As for the partial factors appearing in the equations above, 1.0 can be used as long as the L1 ground motion is concerned.

(c) Anchor

There are several types of anchors for sheet-pile quay walls including plates, sheet piles, vertical piles and coupled piles. An appropriate method for performance verification should be employed depending on the type the anchor.

The location of the anchor has significant effects on the stability of the anchor. An appropriate location should be selected depending on the type of the anchor. In the case of an anchor plate, the active failure plane for the sheet pile starting from the seabed and the passive failure plane starting from the bottom of the plate should not intersect below the ground surface as shown in Figure 23. In the case of a vertical anchor pile, the active failure plane for the sheet pile starting from the seabed and the passive failure plane starting from the $l_{m1}/3$ point of the pile should not intersect below the connection between the tie rod and the pile as shown in Figure 24. In this sentence, l_{m1} is the distance from the top of the pile to the shallowest point with zero moment. The $l_{m1}/3$ point means the point $l_{m1}/3$ deeper than the top of the pile. The location of the anchor sheet pile can be determined in the same way as the vertical anchor pile as long as the anchor sheet pile has sufficient length. In the case of coupled anchor piles, the top of the coupled piles should not be included in the active failure wedge for the sheet pile as shown in Figure 25.

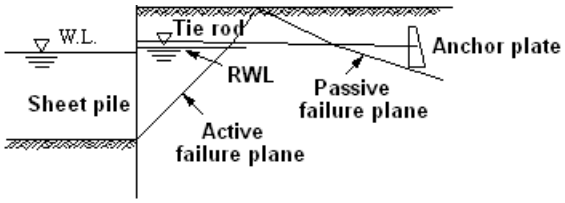

Figure 23 Preferable location of anchor plate.

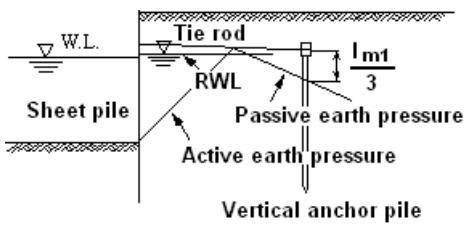

Figure 24 Preferable location of vertical anchor pile.

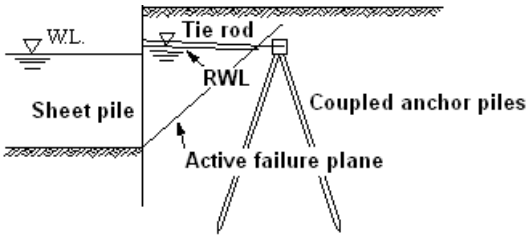

Figure 25 Preferable location of coupled anchor piles.

The stability of an anchor plate can be verified, taking into account the active and passive eath pressures and the force due to the tie rod as shown in Figure 26, using the following inequality.

$$E_{pd} \geq \gamma_a \left(A_{pd} + E_{ad} \right) \tag{44}$$

where

A_p: force due to the tie rod after the correction for the rigidity of the sheet pile (Figure 23)
E_a: active earth pressure resultant acting on the plate
E_p: passive earth pressure resultant acting on the plate
γ_a: structural analysis factor (=2.0)

The design values in the inequality (30) can be obtained from the characteristic values as follows.

$$\begin{aligned} E_{ad} &= \gamma_{E_a} E_{ak} \\ E_{pd} &= \gamma_{E_p} E_{pk} \\ A_{pd} &= \gamma_{A_p} A_{pk} \end{aligned} \tag{45}$$

As for the partial factors appearing in the inequality above, 1.0 can be used as long as the L1 ground motion is concerned.

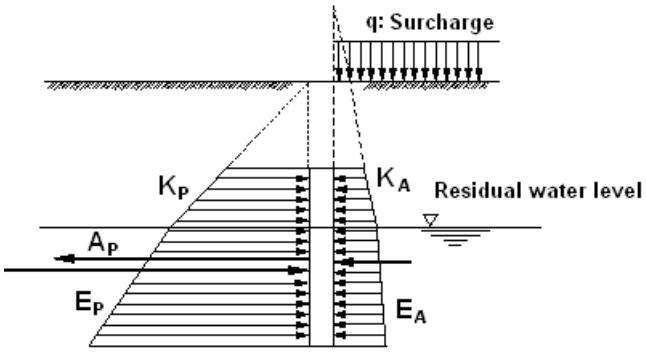

Figure 26 Stability of the anchor plate.

The stress of a vertical anchor pile can be evaluated by modeling the pile as a beam on elastic foundation. The governing equation for a beam on elastic foundation can be written as follows.

$$EI \frac{d^4 y}{d x^4} = - \ p B \tag{46}$$

where

EI: flexural rigidity of the pile
x: depth from the ground surface
y: deflection of the pile
p: subgrade reaction for unit area
B: width of the pile

According to Kubo (1964), the subgrade reaction can be modeled as

$$p = k_s x\ y^{0.5} \tag{47}$$

for the S-type ground and

$$p = k_c\ y^{0.5} \tag{48}$$

for the C-type ground, respectively. The S-type ground can be defined as a ground with SPT N value increases with depth and typically includes sandy soil with uniform density and normally consolidated cohesive soil. The C-type ground can be defined as a ground with uniform SPT N value and typically includes shallow and dense sandy soil and heavily overconsolidated cohesive soil.

The coefficients k_s and k_c should be determined based on in-situ load tests. Once coefficients are obtained, the deflection of the pile subject to the force from the tie rod can be obtained by solving the equation (46) numerically. Then the calculated stress should be compared with the yield stress of the pile. For this verification, partial factors of 1.0 and structural analysis factor of 1.12 can be used as long as the L1 ground motion is concerned.

The procedure described above can be applied to the evaluation of the stability of an anchor sheet pile.

The stability of coupled anchor piles can be evaluated as follows. First of all, the force from the tie rod should be distributed to both piles as Figure 27, following the equation (49).

$$\begin{aligned} P_1 &= \frac{H \cos\theta_2}{\sin\left(\theta_1 + \theta_2\right)} \\ P_2 &= \frac{-H \cos\theta_1}{\sin\left(\theta_1 + \theta_2\right)} \end{aligned} \tag{49}$$

where P_1 and P_2 are the axial forces (compression positive) and θ_1 and θ_2 are the angles shown in Figure 27. Then the axial forces should be compared with the maximum resistance of the soil. For this comparison, structural analysis factor of 1.0 can be used as long as the L1 ground motion is concerned.

The maximum resistance of the soil can be evaluated as follows.

For the compressional axial force, the maximum resistance is the sum of two factors, namely, the pile tip resistance and the friction as follows.

$$R_{td} = R_{pd} + R_{fd} \tag{50}$$

where
R_t :total resistance
R_p :pile tip resistance
R_f :friction

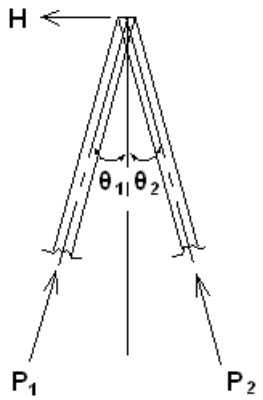

Figure 27 Stability of the coupled anchor piles.

The design values can be obtained from the characteristic values as follows.

$$R_{pd} = \gamma_{R_p} R_{pk}$$
$$R_{fd} = \gamma_{R_f} R_{fk} \quad (51)$$

As for the partial factors appearing in the equation (51), 0.66 can be used. If there is much uncertainty in the pile tip resistance, 0.50 can be used as a partial factor for the pile tip resistance.

The characteristic value of the pile tip resistance can be obtained for sandy soil as

$$R_{pk} = 300\ N\ A_p$$
$$N = \frac{N_1 + \overline{N_2}}{2} \quad (52)$$

where

R_{pk}: characteristic value of the pile tip resistance (kN)

A_p: effective area at the pile tip (m^2)

N_1: SPT N value at the pile tip

$\overline{N_2}$: SPT N value averaged in the layers with the thickness of 4B above the pile tip

B: diameter or width of the pile (m)

For piles with small diameter, the hatched area in Figure 28 can be included in the effective area.

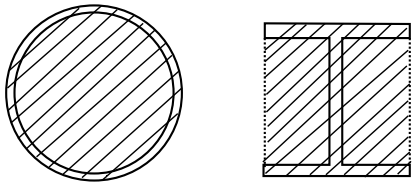

Figure 28 Effective area for piles with small diameter.

The characteristic value of the pile tip resistance can be obtained for cohesive soil as

$$R_{pk} = 6\ c_p A_p \tag{53}$$

where

c_p: cohesion of the soil (kN/m^2)

The characteristic value of the friction can be obtained for sandy soil as

$$R_{fk} = 2\bar{N}A_s \tag{54}$$

where

R_{fk}: characteristic value of the friction (kN)

A_s: contact area between the soil and the pile (m^2)

$\bar{N}$: averaged SPT N value

The characteristic value of the friction can be obtained for cohesive soil as

$$R_{fk} = \overline{c_a} A_s \tag{55}$$

where

$\overline{c_a}$: averaged cohesion of the soil (kN/m^2).

If the cohesion is larger than 100kN/m^2 for one of the layers, the actual cohesion of the layer should be replaced with 100kN/m^2 in calculating the averaged cohesion.

For the tensile axial force, the design value of the maximum resistance of the soil can be obtained from the characteristic value as follows.

$$R_{td} = \gamma_{R_t} R_{tk} \tag{56}$$

In the equation above, R_{tk} is equal to R_{fk} in equation (51)**.** As for the partial factor appearing in the equation (56), 0.40 can be used.

(3) Performance verification with detailed dynamic analysis

The performance of seismic-resistant quay walls of sheet-pile type for the L2 ground motion is most typically evaluated with a two-dimensional effective-stress finite element analysis. The descriptions on the effective-stress analysis for a gravity quay wall apply to the effective-stress analysis for a sheet-pile quay wall. In the case of a sheet-pile quay wall, the initial stress distribution is dependent on the construction process. To conduct accurate dynamic analysis, it is important to employ a method which can reproduce the initial stress distribution accurately.

4. Earthquake Resistant Design of Pile-Supported Wharves

[Ministerial Ordinance] (Performance Requirements for Pile-supported wharves) Article 29 (1) For the L1 ground motion, ordinary functions of pile-supported wharves shall be maintained. (2) For the L2 ground motion, particular functions expected for the pile-supported wharf after the

earthquake shall be recovered within a designated period of time in the case of seismic-resistant pile-supported wharves. In the case of a seismic-resistant pile-supported wharf with higher seismic resistance, particular functions expected for the pile-supported wharf after the earthquake shall be maintained.

4.1 General

[Notification] (Performance Criteria for Pile-supported Wharves)
Article 55
(1) Article 48 applies to the performance criteria of pile-supported wharves for the L2 ground motion where applicable.
(2) For the L1 ground motion, the probability of the stress in the upper structure exceeding the strength of the material should not exceed a prescribed value.
(3) For the L1 ground motion, the probability of the axial force in the piles exceeding the maximum resistance of the soil should not exceed a prescribed value.
(4) For the L1 ground motion, the probability of the stress in the piles exceeding the yield stress should not exceed a prescribed value.
(5) Article 49 and 50 applies to the performance criteria of the retaining walls behind the pile-supported wharves where applicable.

[Commentary]
Performance criteria for pile-supported wharf for the L2 ground motion
a) Special seismic resistant pile-supported wharf (for emergency transportation)
1) The limit of deformation of a special seismic resistant pile-supported wharf (for emergency transportation) should be determined in the same way as that of a special seismic resistant quay wall (for emergency transportation) of gravity type.
2) The stress acting in the upper structure should not exceed the strength of the material.
3) The moment in any pile should not exceed the full plastic moment at two or more depths.
4) The axial force in the pile should not exceed the maximum resistance of the soil.
b) Special seismic resistant pile-supported wharf (for main-line transportation)
The performance criteria for a special seismic resistant pile-supported wharf (for main-line transportation) are the same as those for a special seismic resistant pile-supported wharf (for emergency transportation).
c) Standard seismic resistant pile-supported wharf (for emergency transportation)
1) The limit of deformation of a standard seismic resistant pile-supported wharf (for emergency transportation) should be determined in the same way as that of a standard seismic resistant quay wall (for emergency transportation) of gravity type.
2) The stress acting in the upper structure should not exceed the strength of the material.
3) The moment in the pile should not exceed the full plastic moment at two or more depths at least for one pile.
4) The axial force in the pile should not exceed the maximum resistance of the soil.

4.2 Earthquake Resistant Design of Pile-Supported Wharves with Vertical Piles

[Annex]

(1) Outline of performance verification

A typical cross section of a pile-supported wharf with vertical piles is shown in Figure 29. A recommended procedure for the performance verification of a pile-supported wharf with vertical piles is shown in Figure 30. Performance verification for the L1 ground motion can be carried out with a modified pseudo static approach. Performance verification of seismic-resistant pile-supported wharves for the L2 ground motion

should be carried out with a detailed dynamic analysis.

The access bridge should be prepared for the residual horizontal displacement of the retaining wall due to the earthquake motion. The details of the access bridge should be determined so that the residual horizontal displacement of the retaining wall will not be transmitted to the deck[16].

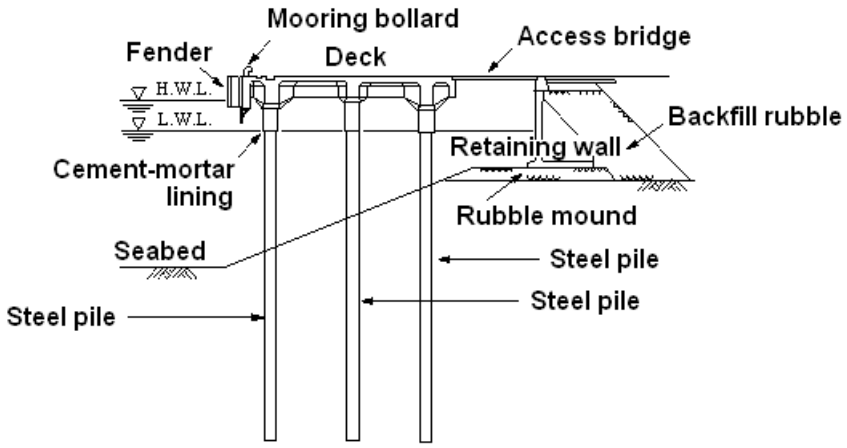

Figure 29 A typical cross section of a pile-supported wharf with vertical piles.

(2) Performance verification with modified pseudo static approach

The modified pseudo static approach described in this section is based on the assumptions that the effect of excess pore water pressure on the performance of the wharf is negligible. Therefore, before using this approach, the engineers should make sure that the effect of excess pore water pressure is negligible. If liquefiable soil is found around the structure, appropriate liquefaction countermeasures should be taken.

In many cases pile-supported wharves are constructed on a slope as shown in Figure 31. In this case, the surface with half the height to the actual ground surface from the seabed is defined as “the virtual ground surface” as shown in Figure 31. When the lateral resistance is evaluated, the soil above the virtual ground surface is neglected. It should be noted, however, that the concept may not be appropriate for a long slope, especially when the deck width is larger than 20 m.

In the modified pseudo static approach, the seismic coefficient for the structure should be calculated with considerations of the dynamic characteristics of the structure. To estimate the seismic coefficient for a pile-supported wharf, the natural period and the damping factor for the pile-deck system is required.

[16] One of the important lessons learned from case histories for port structures in Japan was that the role of an access bridge can be fundamentally important in the seismic performance of a pile-supported wharf. As an example, in the case of Takahama wharf in Kobe Port during the 1995 Hyogo-ken Nanbu earthquake, the horizontal residual displacement of the retaining wall of about 1.5 m was transmitted through the access bridge to the deck and resulted in buckling of the piles. In contrast, in the case of Susaki wharf in Hakata Port during the 2005 West Off Fukuoka Prefecture earthquake, the horizontal residual displacement of the retaining wall of about 0.9 m at maximum was not transmitted to the deck because the land-side support of the bridge was broken, resulting in no significant damage to the pile-deck system (Sugano *et al*., 2007). Thus, the details of the access bridge can affect the seismic performance of the whole structure.

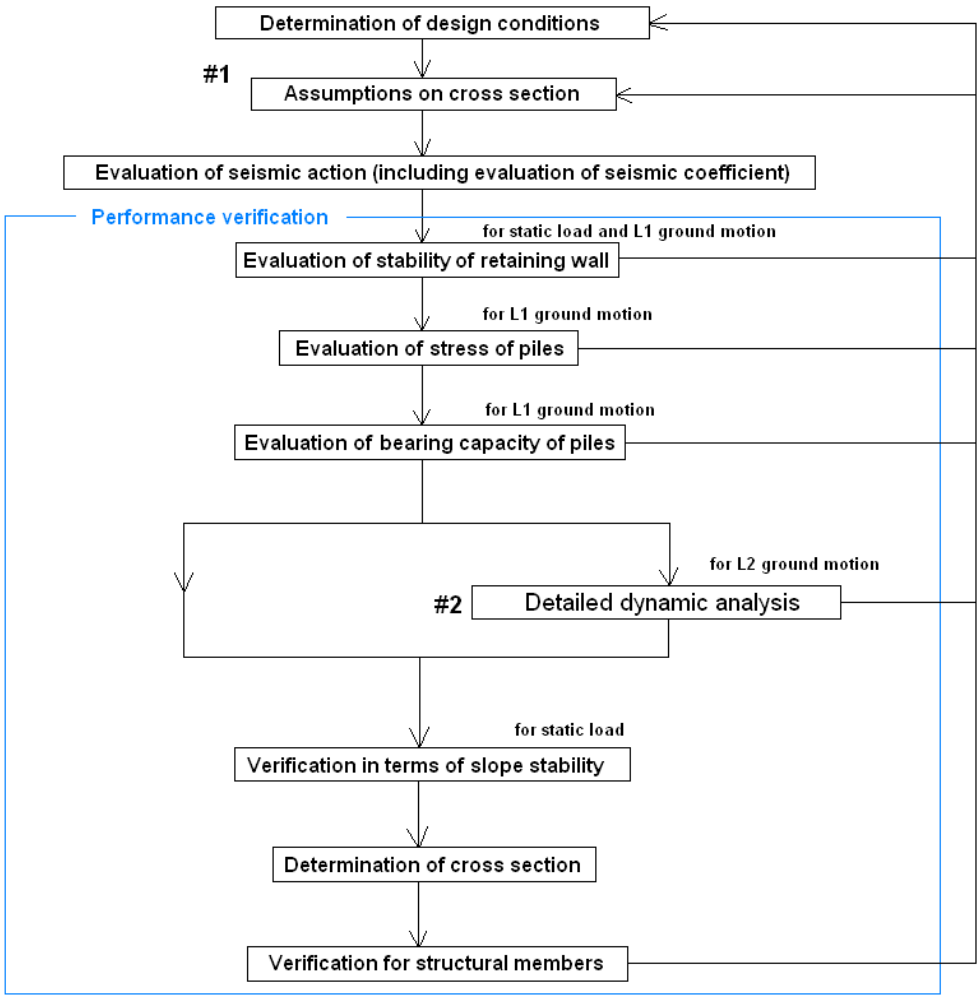

#1 In assuming the cross section, effect of liquefaction should be considered.
#2 For the L2 ground motion, dynamic analysis should be carried out to evaluate residual deformation for seismic resistant quay walls.

Figure 30 Procedure for the performance verification of a pile-supported wharf with vertical piles

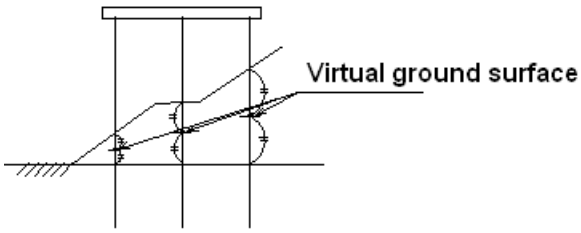

Figure 31 Virtual ground surface

To estimate the natural period of the pile-deck system, it can be assumed that the pile is fixed (both the deflection and the deflection angle is zero) at a depth $1/\beta$ deeper than the virtual ground surface, in which β [17] is defined as

$$\beta = \sqrt[4]{\frac{Bk_{CH}}{4EI}} \tag{57}$$

where

EI : flexural rigidity of the pile
B :width of the pile
k_{CH}: coefficient of subgrade reaction

and k_{CH} is the coefficient defined as

$$p = k_{CH}\, y \tag{58}$$

[17] The left panel of Figure 17.1 shows a pile of a pile-deck system. it is subject to a subgrade reaction below the ground surface and the deflection angle is zero at the top. The deflection of the pile satisfies the following equation.

$$EI\frac{\partial^4 y}{\partial z^4} = 0 \quad \text{(above ground surface)}$$
$$EI\frac{\partial^4 y}{\partial z^4} + B\, k_{CH}\, y = 0 \quad \text{(below ground surface)} \tag{17.1}$$

The solution for this equation which satisfies the boundary conditions can be expressed as follow.

$$y = \frac{(1+\beta h)^3 + 2}{12EI\beta^3}P - \frac{(1+\beta h)P}{4EI\beta}z^2 + \frac{P}{6EI}z^3 \quad \text{(above ground surface)}$$
$$y = \frac{P}{4EI\beta^3}e^{-\beta x}\left\{(1+\beta h)\cos\beta x + (1-\beta h)\sin\beta x\right\} \quad \text{(below ground surface)} \tag{17.2}$$

On the other hand the right panel of Figure 17.1 shows a virtual pile which is fixed at a depth of $1/\beta$. It can be shown that is the moment at the top of the pile is M=(1+ β) P /(2 β) for both piles. Thus the virtual pile is equivalent to the original pile in this sense.

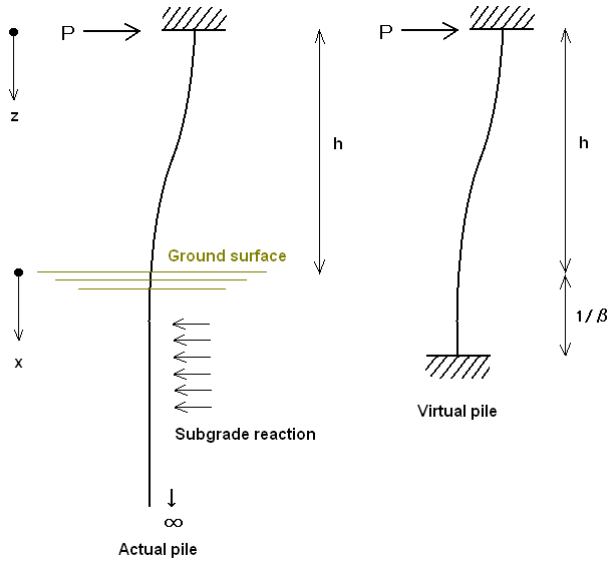

Figure 17.1 Meaning of $1/\beta$

where

y: deflection of the pile
p: subgrade reaction for unit area.

In principle, the coefficient k_{CH} should be determined based on in-situ load tests. When load test data is not available, the following equation can be used to estimate the coefficient.

$$k_{CH} = 1.5\ N \tag{59}$$

where

k_{CH}: coefficient of subgrade reaction (N/cm^3)
N: averaged SPT N value to the depth of $1/\beta$.

It is also reported that the coefficient for the rubble is smaller than that from the equation (59) and it is around 3.0 - 4.0 N/cm^3. Later, when the coefficient is used to evaluate the moment of the pile, the value twice as large as that obtained from the equation (59) can be used.

To evaluating the seismic coefficient for the deck, the L1 ground motion at a depth $1/\beta$ deeper than the virtual ground surface is required. Therefore, 1D earthquake response analysis of ground should be carried out, using the L1 ground motion at the outcrop of a firm ground, to evaluate the acceleration time history at the depth. The acceleration time history can be evaluated for the averaged depth as shown in Figure 32. Using this acceleration time history and the natural period of the pile-deck system, the response acceleration time history of the deck is evaluated (with the damping factor of 0.2). Then the peak response acceleration is divided by the acceleration of gravity to obtain the characteristic value of the seismic coefficient[18]. Basically, the design value of the seismic coefficient can be obtained from the characteristic value as follows.

$$k_{hd} = \gamma_{k_h} k_{hd} \tag{60}$$

If the design value of the seismic coefficient is smaller than 0.05, it should replaced with 0.05. If the design value of the seismic coefficient is larger than 0.25, it should be replaced by the larger of the characteristic value and 0.25.

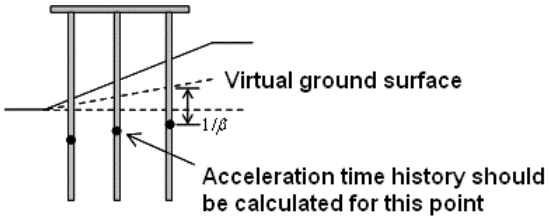

Figure 32 Point where the acceleration time history should be calculated.

The performance verification in terms of the stress of the piles can be based on the following equations.

$$\sigma_{td} + \sigma_{btd} \le \sigma_{tyd} \quad \text{and} \quad -\sigma_{td} + \sigma_{bcd} \le \sigma_{byd} \quad \text{(for tensile axial force)} \tag{61}$$

[18] If the natural period of the pile-deck system is close to the predominant period of earthquake ground motion, the seismic coefficient takes a large value.

$$\frac{\sigma_{cd}}{\sigma_{cyd}} + \frac{\sigma_{bcd}}{\sigma_{byd}} \leq 1.0 \quad \text{(for compressional axial force)} \tag{62}$$

where

σ_t, σ_c: tensile and compressional stress due to axial force
σ_{bt}, σ_{bc}: maximum tensile stress and maximum compressional stress due to bending
σ_{ty}: tensile yield stress
σ_{cy}: compressional yield stress due to axial force for the weak axis
σ_{by}: compressional yield stress due to bending

The design values can be obtained as follows.

$$\sigma_{td} = \frac{P_d}{A},\ \sigma_{cd} = \frac{P_d}{A},\ \sigma_{btd} = \frac{M_d}{Z},\ \sigma_{bcd} = \frac{M_d}{Z} \tag{63}$$

$$\sigma_{tyd} = \gamma_{\sigma_y}\sigma_{tyk},\ \sigma_{cyd} = \gamma_{\sigma_y}\sigma_{cyk},\ \sigma_{byd} = \gamma_{\sigma_y}\sigma_{byk} \tag{64}$$

where

A : cross sectional area of the pile
P : axial force of the pile
Z: section modulus of the pile
M: bending moment of the pile

The partial factors for the verification in terms of the stress of piles can be summarized as Table 3.

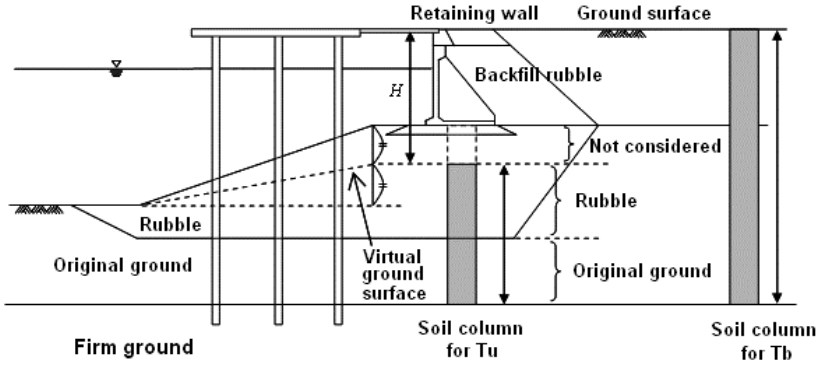

Figure 33 Soil columns from which T_u and T_b should be calculated.

It is a common practice to embed the piles down to a depth of at least $3/\beta$ from the virtual ground surface.

The performance verification in terms of the stability of the retaining wall can be based on the previous descriptions on the stability of a gravity quay wall (the equations 17 - 29), except that the value *b* should be determined to satisfy

$$0.04\ H + 0.08 \leq b \leq 0.08\ H + 0.44 \tag{65}$$

and T_u and T_b should be calculated from the soil columns designated in Figure 33.

Table 3 Partial factors for the verification in terms of the stress of piles.

(a) SKK400

		Special seismic resistant quay wall	Standard seismic resistant quay wall	Others
$\gamma_{\sigma y}$	Yield stress	1.00	1.00	1.00
γ_{kCH}	Subgrade reaction	0.66	0.72	0.80
γ_{kh}	Seismic coefficient	1.68	1.36	1.23
γ_{q}	Surcharge	1.00	1.00	1.00
γ_{a}	Structural analysis factor	1.00	1.00	1.00

(b) SKK490

		Special seismic resistant quay wall	Standard seismic resistant quay wall	Others
$\gamma_{\sigma y}$	Yield stress	1.00	1.00	1.00
γ_{kCH}	Subgrade reaction	0.66	0.72	0.80
γ_{kh}	Seismic coefficient	1.77	1.43	1.30
γ_{q}	Surcharge	1.00	1.00	1.00
γ_{a}	Structural analysis factor	1.00	1.00	1.00

(3) Performance verification with detailed dynamic analysis

The performance of seismic-resistant pile-supported wharves with vertical piles for the L2 ground motion is most typically evaluated with a two-dimensional effective-stress finite element analysis. The descriptions on the effective-stress analysis for a gravity quay wall apply to the effective-stress analysis for a pile-supported wharf with vertical piles. In the case of a pile-supported wharf with vertical piles, spring elements should be installed between the piles and the ground to account for three-dimensional nature of the pile-soil system. The parameters for the spring elements should be determined appropriately, referring to past case histories (*e.g.*, International Navigation Association, 2001).

4.3 Earthquake Resistant Design of Pile-Supported Wharves with Coupled Piles

[Annex]

A typical cross section of a pile-supported wharf with coupled piles is shown in Figure 34. Basically, the descriptions on the performance verification of pile-supported wharves with vertical piles (**4.2**) can be applied to the performance verification of pile-supported wharves with coupled piles. In this section, some exceptions are described.

The stability of coupled piles can be evaluated as follows. First of all, the lateral and vertical forces should be distributed to both piles as Figure 35, following the equation (66).

$$P_1 = \frac{V \sin\theta_2 + H \cos\theta_2}{\sin\left(\theta_1 + \theta_2\right)}$$
$$P_2 = \frac{V \sin\theta_1 - H \cos\theta_1}{\sin\left(\theta_1 + \theta_2\right)} \quad (66)$$

where P_1 and P_2 are the axial forces (compression positive) and θ_1 and θ_2 are the angles shown in Figure 35. Then the axial forces should be compared with the maximum resistance of the soil. The

maximum resistance of the soil can be evaluated based on the previous descriptions on the stability of the coupled anchor piles (the equations 50 - 56).

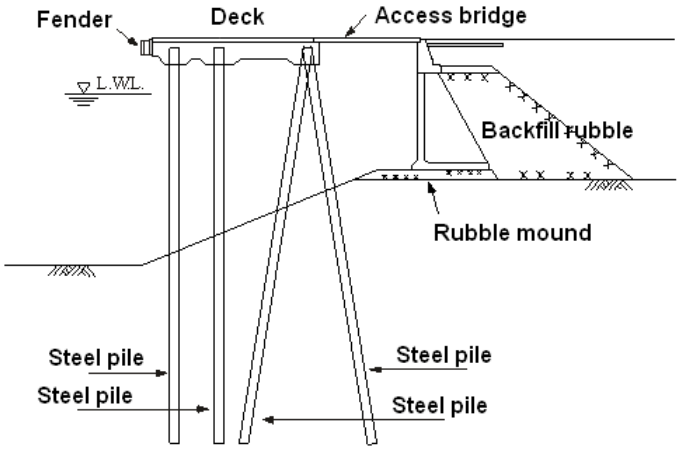

Figure 34 A typical cross section of a pile-supported wharf with coupled piles.

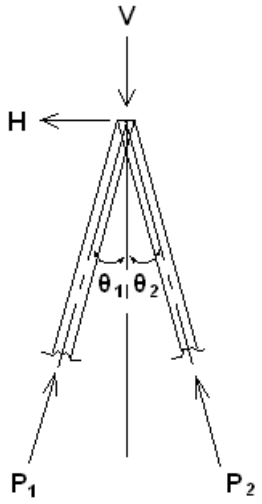

Figure 35 Stability of the coupled piles.

[References]

Aki, K. (1967): Scaling law of seismic spectrum, *J. Geophys. Res.,* Vol.72, pp.1217～1231.

Aki, K. (1966): Generation and propagation of G waves from the Niigata earthquake of June 16, 1964. 2. Estimation of earthquake moment, released energy, and stress-strain drop from G wave spectrum, *Bulletin of the Earthquake Research Institute,* Vol.44, pp.23～88.

Aoi, S., K. Obara, S. Hori, K. Kasahara and Y. Okada (2000): New strong-motion observation network: KiK-net, *Eos Trans. Am. Geophys. Union*, 81, 329.

Brune, J.N. (1970): Tectonic stress and the spectra of seismic shear waves from earthquake, *J. Geophys. Res*., Vol.75, pp.4997～5009.

Brune, J.N. (1971): Correction, *J. Geophys. Res.*, Vol.76, p.5002.

Iai, S., Y. Matsunaga and T. Kameoka (1992): Strain space plasticity model for cyclic mobility, *Soils and Foundations*, Vol.32, No.2, pp.1-15.

Iai, S., K. Ichii, H. Liu and T. Morita (1998): Effective stress analyses of port structures, *Soils and Foundations, Special Issue on Geotechnical Aspects of the January 17, 1995 Hyogoken-Nambu Earthquake,* No.2, pp.97-114.

Ichii, K., S. Iai and T. Morita (1997): Effective stress analyses on the performance of caisson type quay walls during 1995 Hyogokne-Nanbu earthquake, *Report of the Port and Harbour Research Institute*, Vol.36, No.2, pp.41-86 (in Japanese).

Inagaki, H., S. Iai, T. Sugano, H. Yamazaki and T. Inatomi (1996): Performance of caisson type quay walls at Kobe Port, *Special Issue of Soils and Foundations*, pp.119-136.

International Navigation Association (2001): Seismic design guidelines for port structures, Balkema.

Iwata, T. and K. Irikura (1986): Separation of source, propagation and site effects from observed S waves. *Zisin*, 39, pp.579-593 (in Japanese with English abstract).

Kinoshita, S. (1998): Kyoshin Net (K-net), *Seim. Res. Lett.*, 69, pp.309-332.

Kobayashi, M., M. Terashi, K. Takahashi, K. Nakashima and H. Odani (1987): A new method for calculating the bearing capacity of rubble mounds, *Report of the Port and Harbour Research Institute*, Vol.26, No.2, pp.371-411 (in Japanese with English abstract).

Kowada, A., M. Tai, Y. Iwasaki and K. Irikura (1998): Evaluation of horizontal and vertical strong ground motions using empirical site-specific amplification and phase characteristics, *J. Struct. Constr. Eng., AIJ* No.514, pp.97-104 (in Japanese with English abstract).

Kubo, K. (1964): A new method for the estimation of lateral resistance of piles, *Report of the Port and Harbour Research Institute*, Vol.2, No.3, pp.1-37 (in Japanese with English abstract).

Miyake, H., T. Iwata and K. Irikura (2003): Source characterization for broadband ground-motion simulation: kinematic heterogeneous source model and strong motion generation area, *Bulletin of the Seismological Society of America*, Vol.93, pp.2531-2545.

Mizukami, J. and M. Kobayashi (1991): Strength characteristics of rubble mound by large scale triaxial compression test, *Technical note of the Port and Harbour Research Institute*, No.699 (in Japanese with English abstract).

Nozu, A. and W.D. Iwan (2003): Robustness of predominant direction of near-source ground motions and its utilization in port planning, *J. Struct. Mech. Earthquake Eng., JSCE*, No.738/I-64, pp.49-54.

Nozu, A. and T. Nagao (2005): Site amplification factors for strong-motion sites in Japan based on spectral inversion technique, *Technical Note of the Port and Airport Research Institute*, No.1102 (in Japanese with English abstract).

Nozu, A. and T. Sugano (2008): Simulation of strong ground motions based on site-specific amplification and phase characteristics – accounting for causality and multiple nonlinear effects -, *Technical Note of the Port and Airport Research Institute*, No.1173 (in Japanese with English abstract).

Nozu, A., T. Nagao and M. Yamada (2008): A strong motion prediction method suitable for areas with less information on subsurface structure – Kowada's method and its application to shallow crustal earthquakes in Japan, *Proceedings of the 14th World Conference on Earthquake Engineering* (to appear).

Sawada, S., H. Morikawa, K. Toki and K. Yokoyama (1998): Identification of path and local site effects on phase spectrum of seismic motion, *Proceedings of the 10th Japan Symposium on Earthquake Engineering*, pp.915-920.

Somerville, P.G., K. Irikura, R. Graves, S. Sawada, D. Wald, N. Abrahamson, Y. Iwasaki, T. Kagawa, N. Smith and A. Kowada (1999): Characterizing crustal earthquake slip models for the prediction of strong ground motion, *Seismological Research Letters*, Vol.70, pp.59～80.

Sugano, T., Y. Nozue, T. Tanaka, A. Nozu, E. Kohama, H. Hazarika and I. Motono (2007): Damage to port facilities by the 2005 West Off Fukuoka Prefecture earthquake, *Technical note of the Port and Airport Research Institute*, No.1165 (in Japanese with English abstract).

Takahashi, K., Y. Kikuchi and Y. Asaki (1993): Analysis of flexural behavior of anchored sheet pile walls, *Technical note of the Port and Harbour Research Institute*, No.756 (in Japanese with English abstract).

The International Organization for Standardization (2005), Bases for design of structures – seismic actions for designing geotechnical works, ISO23469.

The Japan Ports and Harbours Association (2007): The technical standards and commentaries for port and harbour facilities in Japan (in Japanese).

Yamada, M., Hirai, T., Iwashita, T., Kamae, K. and Irikura, K. (1999): Simulation of ground motion by the modified fault model of the Hyogo-ken Nanbu earthquake, Program and Abstracts, *The Seismological Society of Japan 1999 Fall Meeting*, A14 (in Japanese).